BULETINUL INSTITUTULUI POLITEHNIC DIN IAŞI

Volumul 63 (67)
Numărul 1

Secția
MATEMATICĂ
MECANICĂ TEORETICĂ
FIZICĂ

2017 **Editura POLITEHNIUM**

BULETINUL INSTITUTULUI POLITEHNIC DIN IAŞI
PUBLISHED BY
"GHEORGHE ASACHI" TECHNICAL UNIVERSITY OF IAŞI
Editorial Office: Bd. D. Mangeron 63, 700050, Iaşi, ROMANIA
Tel. 40-232-278683; Fax: 40-232-237666; e-mail: polytech@mail.tuiasi.ro

BULETINUL INSTITUTULUI POLITEHNIC DIN IAŞI
BULLETIN OF THE POLYTECHNIC INSTITUTE OF IAŞI
Volumul 63 (67), Numărul 1 2017

Secția

MATEMATICĂ. MECANICĂ TEORETICĂ. FIZICĂ

SUMAR

BULETINUL INSTITUTULUI POLITEHNIC DIN IAŞI
BULLETIN OF THE POLYTECHNIC INSTITUTE OF IAŞI
Volume 63 (67), Number 1 2017

Section

MATHEMATICS. THEORETICAL MECHANICS. PHYSICS

CONTENTS

BULETINUL INSTITUTULUI POLITEHNIC DIN IAŞI
Publicat de
Universitatea Tehnică „Gheorghe Asachi” din Iaşi
Volumul 63 (67), Numărul 1, 2017
Secţia
MATEMATICĂ. MECANICĂ TEORETICĂ. FIZICĂ

LIQUID CRYSTALLINE PHASE IN BIOLOGICAL PROCESSES

BY

CRISTINA-DELIA NECHIFOR[1,*], MIHAI ANGHELUȚĂ[2], ANA MARIA CIUBARA[3] and DANA ORTANSA DOROHOI[4]

[1]“Gheorghe Asachi” Technical University of Iaşi,
Faculty of Machine Manufacturing and Industrial Management
[2]“Iulius Hațeganu” University of Medicine and Pharmacy, Cluj - Napoca
[3]“Dunărea de Jos” University of Galați,
Faculty of Medicine and Pharmacy
[4]“Alexandru Ioan Cuza” University of Iași,
Faculty of Physics

Received: January 10, 2017
Accepted for publication: February 27, 2017

Abstract. The role of liquid crystals in biological processes is revealed by the model membranes which represent globules containing phospholipids separated by water. The role of lipid concentration, temperature and drugs in the model-membranes fluidity is discussed in this paper. The cholesterol effect on the phospholipid/water systems in controlling the cell membrane fluidity is also evidenced. The influence of Gramicidin S and cholesterol on the model membrane DPPG/water is illustrated by using IR symmetric and asymmetric bands of $–CH_2$ components of the hydrocarbon chains of DPPG.

Keywords: Phospholipids; lyotropic liquid crystals; Cholesterol; membrane fluidity; IR spectra.

[*]Corresponding author; *e-mail*: cristina.nechifor@tuiasi.ro

1. Introduction

The liquid crystalline phases, or mesophases, are distinct states of matter with ordering properties between the high ordered crystals and total disordered liquids (Muscutariu, 1981; Gray, 1962; Brown *et al*., 1971; Brown, 1975). The compounds giving mesophases under suitable conditions are named mesogens.

Liquid crystals can be classified in thermotropic and lyotropic. The main factor influencing the degree of order of thermotropic liquid crystals is temperature. The lyotropic liquid crystals are obtained at a given concentration of the mesogens in thermodynamically bad solvents, by occurrence between hydrophobic and hydrophilic interactions.

Liquids crystals are present now in the highest domains of the Techniques, Informatics, Medicine and so one (Kallard, 1970; Kallard, 1973; Gray and Winsor, 1974; Brown and Volken, 1979). Liquid crystals and the phenomena bonded by them have important implications in biological processes (Gray and Winsor, 1974; Brown and Volken, 1979). The biological membranes whose functions can be explained by their liquid crystallinity with tridimensional order parameter have a crucial role in all cellular phenomena.

The components of the cell membranes include lipids (phospholipids, phosphatidylethanolamines, phosphatidylserines and phosphatidylcholines), proteins, metal-ions, cholesterol and water which mutually interact and are organized in such way that permits the molecules and ions transport between the outer and exterior of the cells. Associated of each lipid class are fatty acids of different chain length and saturation. The lipids which occur in membranes have liquid crystalline properties. They appear to exhibit long range order with certain amount of short range disorder. These properties are relevant for the membranes structure and functionality.

The mosaic structural model (Muscutariu, 1981) of cell membranes in which they are represented as infinite continuous bilayers of lipids and specific proteins, separated by aqueous phases in an instantaneous thermodynamic equilibrium, can be used to explain the mechanisms assuring the membranes functionality, such as: transmission of the nervous impulse; trans - membrane transport; specific effects of hormones and drugs on the biological cells.

The fluidity of the mosaic structure, based on its liquid crystalline properties is also very important for redistribution of the membrane components by translational diffusion through the viscous tridimensional medium.

The amphiphilic components (lipids and proteins) composing the biological membranes do not interact between them; the liquid crystalline order is determined by the interactions between the hydrophilic heads of the amphiphilic constituents with water molecules. In aqueous medium they form a stratified structure (double layers separated by water molecules), resulted from the maximization of hydrophilic interactions and the minimization of the

hydrophobic ones. The double layers are stabilized by specific interactions between ionized heads of the phospholipids and water molecules.

The hydrocarbon chains are oriented out of water contact. Long chains fatty acids esters and glycerides are packed in this way due to the favorable dispersion which arises from parallel packed chains. The stability of the biological membranes is determined by the balance between hydrophobic and hydrophilic interactions of amphiphilic molecules and water.

The biological membrane structure corresponds to the minimum of the free energy determined by the structural features of lipids and proteins and by their interactions with aqueous medium.

The structure of the biological membranes is more complicated than that of the phospholipid double layers, used for simplicity as model-membranes. This very simple model membrane is used to establish some properties bonded to the membrane fluidity as function on temperature, pressure and impurities.

The aim of this study is to emphasize the role of external factors in modifying the cell membrane fluidity by making as model the DPPC/water or DPPC derivatives/water systems.

2. External Factors Influencing the Membrane Fluidity

The liquid crystalline nature of biological membranes facilitates modifications in its fluidity under the external factors. Lyotropic liquid crystals are primarily influenced by the lipid concentration in the polar solvent (in biological processes the polar solvent is water). Temperature, pressure and the drug presence can also influence the membrane fluidity and so, their functionality.

The behavior of DPPC (dipalmitoylphosphatidylcholine) in water has been summarized by D. Chapman (Chapman 1974; Chapman *et al.*, 1967) in a diagram alike that from Fig. 1. In the gel phase (Chapman, 1974) water separates the double layers of lipids with their hydrocarbon chains in a hexagonal lattice.

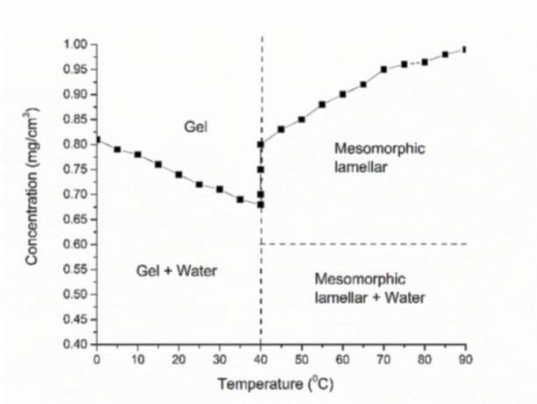

Fig. 1 − Phase diagram of DPPC/water system.

From the phase diagram of DPPC/water system (Fig. 1) it results that after the main phase transition (t > 42ºC), the ability of lipids to disperse in water increases and the system gel + water passes in mesomorphic lamellar phase + water. For lipid concentration higher than 0.6 and t > 42ºC, water is eliminated from the mesomorphic system of DPPC/water. At high temperatures and in the presence of small quantities of water, the cubic phase occurs (C < 0.8 and T < 40ºC).

At small temperatures, water separates the double layers of lipids and their hydrocarbon chains are packed in organized crystalline manner. When water content increases, temperature of endothermic transition decreases. The decrease is not indefinite; for DPPC it ranges up to 42ºC. It was explained that water can produce loosing of the ionic structure of the lipid heads causing reduction of the dispersive forces between the hydrocarbon chains.

Some biological membranes can exhibit the main phase transition many degrees below the biological environmental temperature. So, these membranes can be in a high mobile and fluid condition at biological environmental temperature. These conditions are realized especially in the case of highly unsaturated lipids.

The drug presence can decrease the main phase transition, as it was shown for the DPPC model membrane (Stan *et al*., 2006; Severcan *et al*., 2008).

3. Physico-Chemical Methods in Study of the Liquid Crystalline Phase

Thermotropic mesomorfism of lipid molecules can be evidenced by optical and spectroscopic means.

Optics of the thin films of lipids shows that: they are birefringent when are viewed between crossed polarizers; they loss birefringence by heating below the phase transition temperature and they completely loss birefringence at the melting point.

For example, dimystiroylphosphatidylethanolamine (DMOPEA) (Chapman, 1974) at room temperature is birefringent and after heating near its first transition temperature (120ºC) it was emphasized small decrease of its birefringence. After this temperature, near the melting point (200ºC), the birefringence is definitely lost.

When the lipid temperature is near the temperature of the main phase transition, the IR spectrum (Chapman *et al*., 1967), undergoes remarkable changes and loss all the fine structure and the details from the lower temperature. For temperatures higher than the main phase transition temperature, the IR spectrum is then similar with that obtained with phospholipids dissolved in a solvent such as chloroform.

The differential thermal analysis shows that a marked endothermic transition (with heat absorption) occurs near 120ºC. After this temperature the system DMOPEA/water becomes fluid (Chapman and Collin, 1965).

The phase transition is primarily concerned with the hydrocarbon chains of the phospholipids (evidenced by X-ray, IR and PMR spectra). The trends in the transition temperatures also confirm that the phase transition is primarily associated with the melting of the hydrocarbon chains of the phospholipids directly correlated with the dispersion forces between the hydrocarbon chains.

4. Results and Discussions

DSC and DTA are also used in establishing the membranes fluidity.

The transition temperature for different phospholipids classes differ even though they contain exactly the same fatty acid residues (Fig. 2) (Chapman and Collin, 1965).

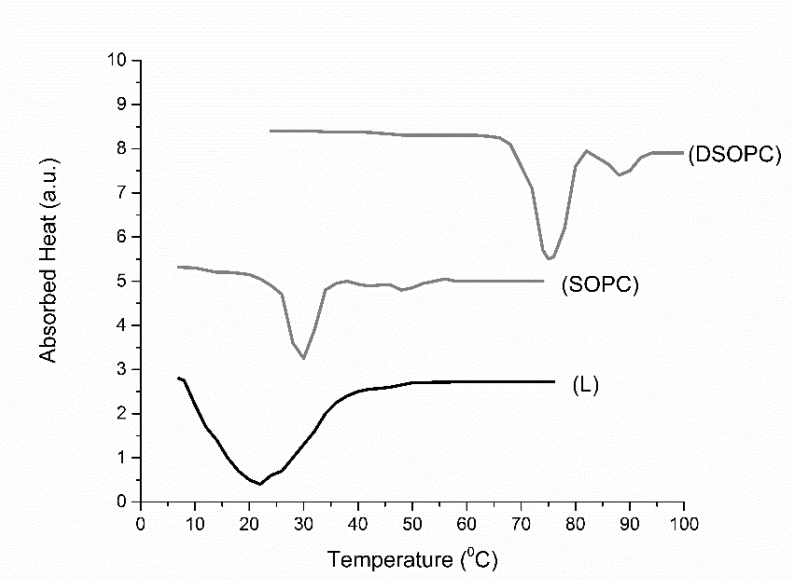

Fig. 2 – Differential thermal analysis (DTA) heating curves for some phospholipids: (L) – egg yolk lecithin; (SOPC) 1- stearoyl-2-oyl-DL-phosphatidylcholine; (DSOPC) 1,2- Distearoyl-DL-phosphatidylcholine.

Phospholipids having exactly the same fatty acid residues are characterized by different transition temperature, as it results from Fig. 2 for SOPC and DSOPC. The egg yolk lecithin (L) is a mixture of phospholipids, but it has only a main point transition, at a temperature smaller than its components.

The high saturated derivatives exhibit transition temperatures much higher than the room temperature, while the natural phospholipids from erythrocytes or mitochondrial membranes contain large numbers of unsaturated cis-double bonds, and therefore, in dry conditions, have endothermic transition temperature either near or below the room temperatures.

At the first termothropic transition temperature, the molecular motion of the chains increases until the first transition point; lateral expansion of the crystal lattice is forced to take place. This expansion allows even greater chain mobility, possible involving cooperative motion of the chains with rotation about C-C bonds.

Near the endothermic transition temperature, a given phospholipid can be in a highly mobile condition, with its hydrocarbon chains flexing and twisting. The more unsaturated the chains, the lower is the main phase transition temperature at which this phenomenon occurs.

In natural membranes the interactions with other molecules can produce inhibition of the chain motion. Due to less perfect packing arrangements, at environmental temperatures, even greater mobility of the chains of the lipid and indeed of the whole lipid molecules could be expected.

When phospholipids are examined in the presence of increasing amounts of water, the various physical-chemical techniques (IR, DSC, NMR, Raman) show that as the amount of water increases, the marked endothermic transition temperature for a given phospholipid falls (Fig. 3).

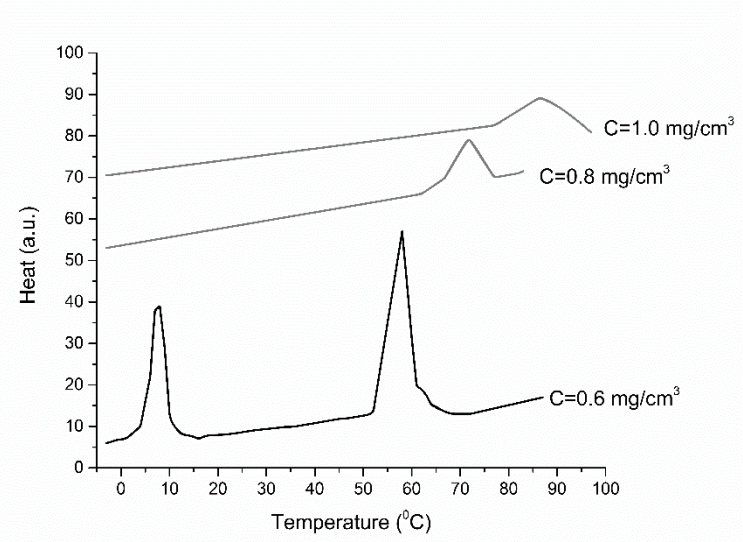

Fig. 3 – DSC heating curves of 1,2 Stearoylphosphatidylcholine (SOPC) in water at different phospholipid concentrations: C = 0.6; 0.8 and 1.0 mg/cm^3.

In the presence of increasing amounts of water, the main phase transition temperature of phospholipids decreases due to water addition to the head of amphiphilic molecules, which causes the reduction of the dispersive forces between the phospholipid chains.

The transition temperature does not fall indefinitely; it reaches a limiting value independent of the water content.

The decrease in the main transition temperature is limited by the energy required to counteract the dispersion forces between hydrocarbon chains necessary to determine the chain melting. The values of the main phase transition temperature are determined by the saturation degree of phospholipids; it is lower for the unsaturated phospholipids. At the biological environmental temperature, the unsaturated phospholipids composing the biological membranes are in highly mobile and fluid conditions.

The natural phospholipids extracted from biological membranes usually exhibit phase transition crystalline – liquid crystalline phases at many degrees below the biological environmental temperature, at which one expects the phospholipids containing unsaturated chains to be in a highly mobile and fluid conditions.

5. The Role of Cholesterol in Biological Membranes

The ability of lipids to disperse in water increases markedly above the main phase transition temperature (Gray and Winsor, 1974; Brown and Volken, 1979).

The drugs can decrease the main phase transition temperature of phospholipids. There are important studies to sustain this affirmation. For example, Gramicidin S (Severcan *et al*., 2008, Stan *et al*., 2006) added to a model membrane of DPPG in water decreases the main phase transition temperature with about 1.5ºC (see Figs. 4, 5 and Table 1).

The interaction of cholesterol with phospholipids is of a great biological importance. Cholesterol occurs in many membranes, particularly in myelin sheaths, or in red blood cell membranes. Cholesterol is solubilized by phospholipids; it has vehicular possibilities. The effect of cholesterol is to disrupt the ordered array of the hydrocarbon chains of the lipids in the gel phase. The presence of cholesterol in mixtures phospholipids/water determines a relative "lipid fluidization".

When cholesterol is added to a model-membrane made by DPPG in water, it decreases the main transition temperature of phospholipid with about 2.5^0C (see Figs. 4, 5 and Table 1). Cholesterol has condensing effect on phospholipids, diminishing the area occupied by the fatty acids.

In Figs. 4 and 5 are given the IR symmetric and asymmetric bands of $-CH_2$ components of the hydrocarbon chains of DPPG as function of temperature for DPPG/water membranes and also for the DPPG/water membranes containing Gramicidin S (GS) and cholesterol (Ch).

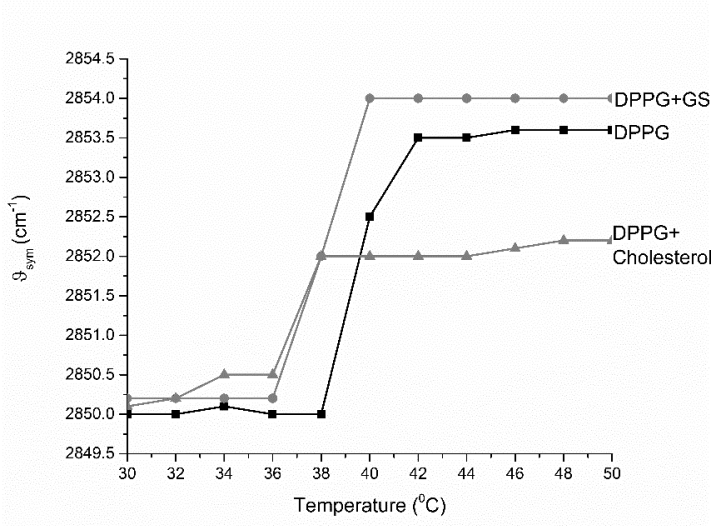

Fig. 4 – Symmetric IR bands of -CH_2 components of the hydrocarbon chains of DPPG in model membranes containing Gramicidin S and Cholesterol.

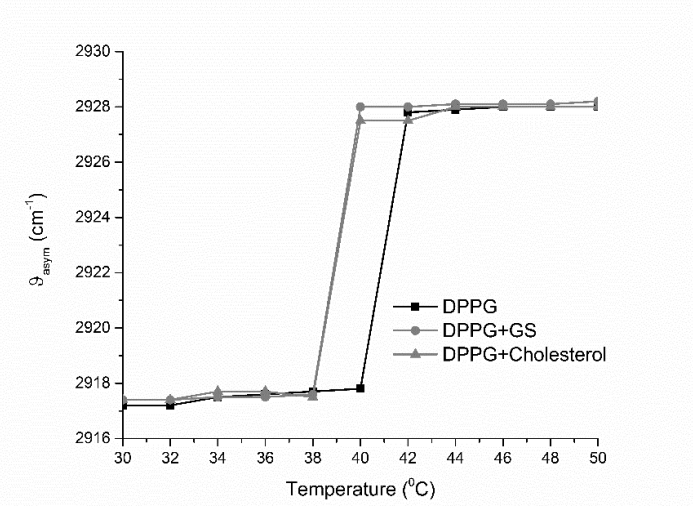

Fig. 5 – Asymmetric IR bands of -CH_2 components of the hydrocarbon chains of DPPGin model membranes containing Gramicidin S and Cholesterol.

The cholesterol presence causes the hydrocarbon chains of different phospholipid molecules to be in an "intermediate fluid" condition. When cholesterol and lecithin are present in equimolar ratios, all the hydrocarbon chains are in a fluid condition. The mixture becomes dispersible in water over a much wider temperature range than occurs with the individual phospholipids (Stewart, 1974).

Table 1
Transition Temperatures of DPPG Model Membranes with Gramicidin S and Cholesterol

Sample	Transition temperature CH_2Symmetric IR band [ºC]	Transition temperature CH_2 asymmetric IR band [ºC]
DPPG	40	41
DPPG+Gramicidin S	38.5	39
DPPG+Cholesterol	37.5	38

The effects of cholesterol in membranes is to control the fluidity of the hydrocarbon chains of the phospholipids providing a coherent structure stable over a wide temperature range and permitting some latitude of the fatty acid content of the component lipids.

6. Conclusions

The main components of the cell membranes are phospholipids and proteins. Their liquid crystalline behavior in water is a determinant factor for the cell membranes functionality.

The liquid crystalline phase of the phospholipids is very important for biological processes due to the fact that assures the permeability of the cell membranes for the ion and molecule transport inside and outside of the cells.

The cell membranes fluidity is influenced by temperature, by some drugs and also by cholesterol.

REFERENCES

Brown G.H., Doane J.N., Neff V.D., *Structure and Physical Properties of Liquid Crystals*, Butterworth, London, 1971.

Brown G.H., *Advances in Liquid Crystals*, Acad. Press, New York, Vol. I 1975; Vol. II 1976; Vol. II 1978; Vol. IV 1979; Vol. V, 1980.

Brown G.H., Volken J.J., *Liquid Crystals and Biological Structures*, Acad. Press, New York, 1979.

Chapman D., Collin D.T., *Nature*, London, **206**, 189-191 (1965).

Chapman D., Williams R.M., Ladbrooke B.D., *Chem. Phys. Lipids*, **1**, 445-475 (1967).

Chapman D., *Significance of Liquid Crystals in Biology*, in: Liquid Crystals and Plastic Crystals, Physico-Chemical Properties and Methods of Investigation, Eds. G.W. Gray and P.A. Winsor, Ellis Horwood Limited-Chichester Halsted Press - a Division of John Willey and Sons Inc., New York, London, Sidney, Toronto, Vol. 2, 1974.

Gray G.W., *Molecular structures and the properties of liquid crystals*, Acad. Press, New York, 1962.

Gray G.W., Winsor P.A., *Liquid Crystals and Plastic Crystals*, Vol. I and II, Halsted Press, New York, 1974.
Kallard T., *Liquid Crystals and their Applications*, Optosonic Press, New York, 1970.
Kallard T., *Liquid Crystal Devices*, Optosonic Press, New York, 1973.
Muscutariu I., *Cristale lichide și aplicații*, Edit. Tehnica, București, 1981.
Severcan F., Agheorghiesei C., Dorohoi D.O., *Rev. de Chim. București*, **59**, *3*, 356-359 (2008).
Stan C., Cristescu R., Severcan F., Dorohoi D.O., *Mol. Cryst. Liq. Cryst*, **457,** 27-41 (2006).
Stewart G.T., *The Role of Liquid Crystals in Life Processes*, Cpt.6.2 in Liquid Crystals and Plastic Crystals, Vol. II, (Editors. G.W. Gray, P.A. Winsor), Halsted Press, New York, 1974.

FAZA CRISTALINĂ LICHIDĂ ÎN PROCESELE BIOLOGICE

(Rezumat)

Rolul cristalelor lichide în procesele biologice este pus în evidență de modelele membranelor reprezentate sub formă de globule care conțin fosfolipide separate de apă. În această lucrare este discutat rolul concentrației lipidelor, temperaturii și a unor medicamente în studiul fluidității membranelor. Un aspect important pus în evidență este efectul colesterolului asupra fluidității sistemelor formate din fosfolipide și apă. Influența Gramicidinei S și a colesterolului asupra membranelor DPPG/apă este ilustrată prin utilizarea benzilor de vibrație simetrică și antisimetrică în IR ale -CH2 ce sunt componente ale lanțurilor de hidrocarburi din DPPG.

BULETINUL INSTITUTULUI POLITEHNIC DIN IAŞI
Publicat de
Universitatea Tehnică „Gheorghe Asachi” din Iaşi
Volumul 63 (67), Numărul 1, 2017
Secţia
MATEMATICĂ. MECANICĂ TEORETICĂ. FIZICĂ

OPTIMIZATION OF THE SYNTHESIS REACTIONS OF SOME NEW THIOSEMICARBAZIDES DERIVED FROM 5-NITROINDAZOLE

BY

CORINA CHEPTEA[1], ANDREEA CELIA BENCHEA[2], MARIN ZAGNAT[1,*], NELA BIBIRE[3], VALERIU ŞUNEL[4] and DANA ORTANSA DOROHOI[2]

[1]“Grigore T. Popa” University of Medicine and Pharmacy, Iaşi,
Faculty of Biomedical Bioengineering
[2]“Alexandru Ioan Cuza” University,
Faculty of Physics
[3]“Grigore T. Popa” University of Medicine and Pharmacy, Iaşi,
Faculty of Pharmacy
[4]“Alexandru Ioan Cuza” University of Iaşi,
Faculty of Chemistry

Received: January 26, 2017
Accepted for publication: March 5, 2017

Abstract. New thiosemicarbazides derived from 5-nitroindazole with biological activity were synthesised. The 5-nitroindazol-1-yl formylhydrazide was treated with various aromatic isothiocyanates in order to obtain new thiosemicarbazides. The conditions in which the reactions take place with the highest yield were established. The optimization reactions were realized in a 3^2 factorial experiment. Some physico-chemical properties of the new synthesized compounds were theoretically established by using HyperChem 8.6.0. The chemical structure of the new synthesized compounds was confirmed by elemental and spectral analysis (FT-IR, ^{1}H-NMR). The new compounds were tested from the toxicity point of view.

Keywords: 5-nitroindazole derivatives; elemental and spectral analyses; factorial experiment for optimization; QSAR parameters.

[*]Corresponding author; *e-mail*: marin.zagnat@umfiasi.ro

1. Introduction

The observation that compounds like thiosemicarbazides have an essential role in the structure and function of certain molecules of importance from a biological point of view, was only the begining for the search of such compounds with significant pharmacological application.

The various references seem to indicate that indazole molecule has a wide range of biological properties, like hepatoprotective (Berhe *et al*., 2010), anti-angiogenic (Huang *et al*., 2010), anti-inflamatory and analgesic (Ribeira *et al*., 2010), antibacterial (Rodriquez *et al*., 2009), citostatic (Yakaiah *et al*., 2007) as well as tuberculostatic (Cheptea *et al*., 2009) activity.

The research showed the importance of the thiosemicarbazides in the composition of drugs with antibacterial (Plech *et al*., 2011; Liesen *et al*., 2010; Shelke *et al*., 2010; Bhat *et al*., 2009), tuberculostatic (Moise *et al*., 2009; Bukovski *et al*., 1998; Ulusoy, 2002), antifungal (Fahmy, 2001) and cytostatic (Seleeman *et al*., 2005; El-Asmy *et al*., 2009) activities.

The aim of this study was to establish the most convenient conditions for synthesis reaction in factorial experiments with temperature and time of reactions considered as relevant variable and to perform a quantum mechanical characterization for the new compounds.

Some physico-chemical properties of the new thiosemicarbazides derived from 5-nitroindazole were theoretically estimated by using HyperChem 8.0.6 program (www.hyperchem.com). The toxicity potential of the obtained compounds was experimentally determined.

2. Experimental

2.1. Materials and Method

All reagents were used as purchased (Sigma-Aldrich, Merk, Fluka, S.C. Chemical Company SA). FT-IR spectra were recording using a FT-IR spectrophotometer (ATR) Brucker Tensor-27; ^{1}H-NMR analysis was performed on a Brucker ARX400 spectrometer (5 mm QNP probe; 1H/13C/31P/19F) and elemental analysis – on an Exeter Analytical CE 440 elemental analyser. The melting points of the obtained compounds were determined with a Mel-Temp melting point module, provided with a digital thermometer.

2.2. Synthesis of 2-[(5'-nitro-1H-indazol-1'-yl)-carbonyl]-N-arillhydrazincarbothioamide (III-VIII)

In a flask equipped with ascending refrigerator, in 100 mL absolute methyl alcohol 0.005 moles hydrazide are introduced. The resulting solution is mildly heating and stirring until becomes clear. In the next step, 0.005 moles different

isothiocyanates in 5 mL absolute methyl alcohol are added. The mixture was refluxed on water bath for 3 h separating an abundant precipitate. This was filtered in vacuum, was dried and finally purified by recrystalization from methyl alcohol.

3. Results and Discussions

The synthesis of the new compounds was performed in several steps. In the first step, the ethyl ester of 5-nitroindazol-1'-il-formic acid was prepared through condensation of 5-nitroindazole with ethyl chloroformate, in the presence of sodium ethoxide, on refluxing in absolute ethyl alcohol.

In the next step, by treating the ester (I) with hydrazine hydrate 98% solution in anhydrous ethanol, the hydrazide of the 5-nitroindazol-formic acid (II) was obtained like a crystalline product after recrystallization from ethyl alcohol (Cigu *et al*., 2014) (Scheme 1).

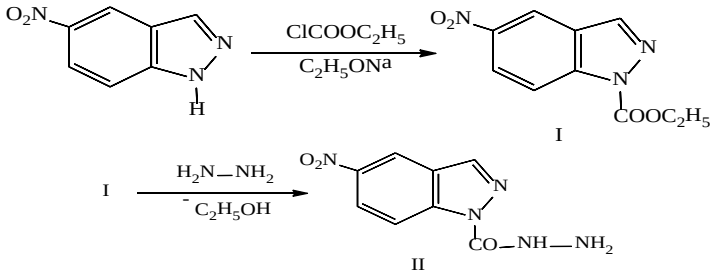

Scheme 1 – Synthesis of the hydrazide of the 5-nitroindazolyl-1-yl-formic acid (II).

Further, the 5-nitro-1H-indazol-1-carboxhydrazide (II) was treated with phenyl-, p-tolyl, p-metoxyphenyl, p-bromophenyl, p-chlorophenyl- and p-iodophenyl-isothiocyanate in absolute ethyl alcohol on reflux for two hours, leading to new 2-[(5'-nitro-1H-indazol-1'-yl)-carbonyl]-N-arilhydrazincarbothioamide (thiosemicarbazides) (III – VIII) (Scheme 2).

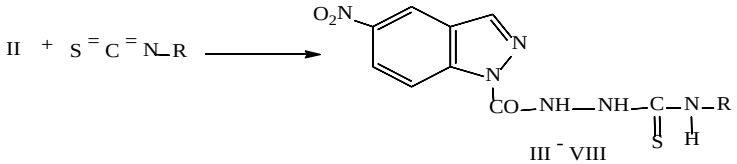

III - VIII

III R = - C_6H_5
IV R = - C_6H_4 - CH_3
V R = - C_6H_4 - OCH_3
VI R = - C_6H_4 - Br(p)
VII R = - C_6H_4 - Cl(p)
VIII R = - C_6H_4 - I(p)

Scheme 2 – Synthesis of the new thiosemicarbazides (III-VIII).

3.1. Mathematical Modeling of Optimization Reactions

A 3^2 factorial experiment (Fisher, 1996; Azzouz, 1998) was organized for each reaction. The chemical reactions were made in a short variation domain of relevant variables in order to estimate the maximum of the reaction yield. Two relevant variables – temperature and reaction time – were considered being significant for the reaction yield (Table 1).

The real and the a-dimensional relevant coordinates are listed in Table 1 in which the measured yields in factorial experiments are also listed.

Table 1
Real (X_1, X_2) and a-Dimensional (x_1, x_2) Variables and Reaction Yield (η) in 3^2 Factorial Experiments

x_1 (X_1 °C)	x_2 (X_2 min)	η_{III} [%]	η_{IV} [%]	η_{V} [%]	η_{VI} [%]	η_{VII} [%]	η_{VIII} [%]
-1 (55)	-1(105)	79	82	75	74	76	78
-1 (55)	0 (120)	81	84	77	80	81	80
-1 (55)	1 (135)	80	83	74	78	77	79
0 (60)	-1 (105)	79	84	77	78	78	79
0 (60)	0 (120)	83	87	79	81	82	83
0 (60)	1 (135)	82	85	78	79	79	80
1 (65)	-1 (105)	80	83	76	75	78	78
1 (65)	0 (120)	82	86	78	80	81	82
1 (65)	1 (135)	81	84	77	79	79	80

The dependence of the reaction yield on the a-dimensional variables x_1 and x_2 was considered of the type:

$$\eta = a_0 + a_1 x_1 + a_2 x_2 + a_{12} x_1 x_2 + a_{11} x_1^2 + a_{22} x_2^2 \quad (1)$$

The coefficients a_0, a_1....a_{22} of Eq. (1) for each compound, obtained by statistical method (Moise *et al*., 2010; Hurjui *et al*., 2012), are listed in Table 2.

Table 2
Regression Coefficients in Reaction (1) Obtained in Factorial Experiments

Compound	a_0	a_1	a_2	a_{12}	a_{11}	a_{22}
III	82.56	0.50	0.83	0	-0.83	-1.84
IV	86.78	0.67	0.50	0	-1.67	-2.17
V	79.11	0.83	0.17	0.50	-1.83	-1.83
VI	81.40	0.33	1.67	0	-1.67	-3.14
VII	81.66	0.55	0.48	0	-0.95	-2.95
VIII	82.27	0.32	0.58	0.18	-1.15	-2.25

The conditions for extremum values of the yield:

$$\frac{\partial \eta}{\partial x_1} = 0 \quad \text{and} \quad \frac{\partial \eta}{\partial x_2} = 0 \tag{2}$$

were used in order to determine the coordinates (x_{1e}, x_{2e}) corresponding to the extremum of the reaction yield. The sign minus of the coefficients a_{11} and a_{22} in Table 2 shows that the obtained extremum is a maximum (Cheptea *et al*., 2012).

The absolute values of the determined coefficients listed in Table 1 provide information on the intensity of individual effects (coefficients a_1 and a_2) or on the combined effects (a_{12}), of the temperature (x_1) and reaction time (x_2).

The signs (+) or (-) indicate if the variable which multiplies the corresponding coefficient favors or does not favor, respectively, the result of the chemical reaction. In order to determine the accuracy *P* of the experiments, new measurements were made in the center of the small range (Table 3) in which the maxima appeared.

Table 3
Reaction Yield η_c in Central Range of the 3^2 – Factorial Experiments and Accuracy (P, [%]) *of Determinations*

Compound	η_{c1} [%]	η_{c2} [%]	η_{c3} [%]	η_c [%]	P [%]
III	83.5	84.0	83.6	83.7	8.8
IV	87.7	88.0	87.8	87.8	7.5
V	78.7	79.0	78.9	78.9	5.2
VI	81.3	81.5	81.7	81.5	7.1
VII	81.5	81.7	81.8	81.7	5.2
VIII	82.5	82.3	82.20	82.3	5.2

t – Student parameters for the organized experiments were computed by using relation (3).

$$t_j = \frac{|a_j|}{P} \tag{3}$$

The values of the *t*-student parameters listed in the Table 4 attest the significance of the values of the yield in the organized experiments.

Table 4
t-Student Coefficients Obtained in Factorial Experiments for Obtaining the Studied Compounds

Compound	t_j – Student coefficients					
	a_0	a_1	a_2	a_{12}	a_{11}	a_{22}
III	938.20	5.68	9.43	0	9.43	20.91
IV	1157.07	8.93	6.67	0	22.27	28.93
V	1521.35	15.96	3.27	9,62	35.19	35.19
VI	1146.48	4.65	23.52	0	23.52	44.23
VII	1570.38	10.58	9.23	0	18.27	56.73
VIII	1582.11	6.15	11.15	3,46	22.12	43.27

The relations in which the reaction yield is expressed by relevant variables and by their products are the following:

$$\eta_{\mathrm{III}} = 82.56 + 0.50x_1 + 0.83x_2 + 0x_1x_2 - 0.83x_1^2 - 1.84x_2^2 \quad (4)$$

$$\eta_{\mathrm{IV}} = 86.78 + 0.67x_1 + 0.50x_2 + 0x_1x_2 - 1.67x_1^2 - 2.17x_2^2 \quad (5)$$

$$\eta_{\mathrm{V}} = 79.11 + 0.83x_1 + 0.17x_2 + 0.50x_1x_2 - 1.83x_1^2 - 1.83x_2^2 \quad (6)$$

$$\eta_{\mathrm{VI}} = 81.40 + 0.33x_1 + 1.67x_2 + 0x_1x_2 - 1.67x_1^2 - 3.14x_2^2 \quad (7)$$

$$\eta_{\mathrm{VII}} = 81.66 + 0.55x_1 + 0.48x_2 + 0x_1x_2 - 0.95x_1^2 - 2.95x_2^2 \quad (8)$$

$$\eta_{\mathrm{VIII}} = 82.27 + 0.32x_1 + 0.58x_2 + 0.18x_1x_2 - 1.15x_1^2 - 2.25x_2^2 \quad (9)$$

The dependences of the reaction yield of the compounds III-VIII on the relevant variables are illustrated in Figs. 1 *a-f*. In this figures the *a*-dimensional variables x_1 and x_2 vary between [-1, +1].

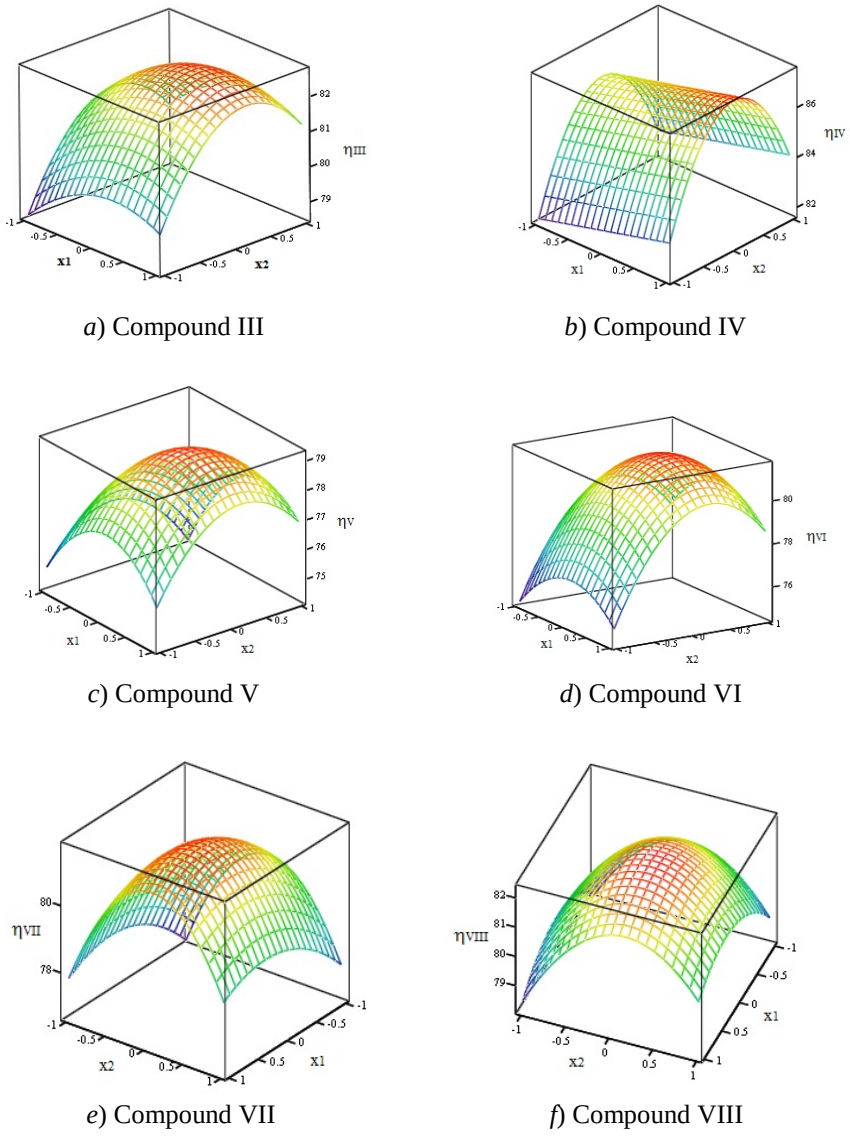

a) Compound III *b*) Compound IV

c) Compound V *d*) Compound VI

e) Compound VII *f*) Compound VIII

Fig. 1 – Three dimensional representation of the compounds III-VIII reaction yield *vs.* the adimensional temperature and time of the chemical reaction.

3.2. Elemental and Spectral Analysis

The structure of compounds III – VIII was confirmed by the results of elemental and spectral (FT-IR, ^{1}H-NMR) analyses.

Synthesis of 2-[(5'-nitro-1H-indazol-1'-yl)-carbonyl]-N-phenylhydrazincarbothioamide (III)

White yellowish solid, yield 81%, m.p.=158 – 160ºC, M=356

Anal. calc. for $C_{15}H_{12}N_6O_3S$; C% 50.56; H% 3.37; N% 23.59; S% 8.98. Found: C% 50.71; H% 3.59; N% 23.76; S% 9.12.

IR (ν, cm^{-1}): 3091 (NH); 1611 (CO); 747 (CHAr); 1129 (C=S); 1331 (NO_2 sym.); 1536 (NO_2 asym.).

^{1}H-NMR (DMSO-d6, 400 MHz), δ (ppm): 7.17-7.19 (d, 1H, CHAr); 7.33-7.40 (m, 4H, CHAr); 7.70-7.74 (d, 1H, CHAr); 8.03-8.05 (d, 1H, CHAr); 8.21 (S, 1H, CHAr); 8.39 (s, 1H, CHAr); 9.69-9.73 (d, 2H, NH); 10.50-10.57 (d, 1H, NH).

Synthesis of 2-[(5'-nitro-1H-indazol-1'-yl)-carbonyl]-N-(p-tolyl)-hydrazin carbothioamide (IV)

White solid, yield 86 %, m.p.=159 – 161ºC, M=370

Anal. calc. for $C_{16}H_{14}N_6O_3S$; C% 51.89; H% 3.78; N% 22.70; S% 8.64. Found: C% 52.08; H% 3.99; N% 22.92; S% 8.89.

IR (ν, cm^{-1}): 3093 (NH); 1698 (CO); 753, 789 (CHAr); 1231 (C=S); 1346 (NO_2 sym.); 1529 (NO_2 asym.).

^{1}H-NMR (DMSO-d_6, 400 MHz), δ (ppm): 2.32 (s, 3H, CH_3); 7.19-7.21 (d, 2H, CHAr); 7.27-7.29 (d, 2H, CHAr); 7.83-7.85 (d, 1H, CHAr); 8.34-8.36 (d, 1H, CHAr); 8.47 (s, 1H, CHAr); 8.90 (s, 1H, CHAr); 9.73-9.76 (d, 2H, NH); 10.52-10.58 (d, 1H, NH).

Synthesis of 2-[(5'-nitro-1H-indazol-1'-yl)-carbonyl]-N-(p-metoxiyphenyl)-hydrazincarbothioamide (V)

White solid, yield 78%, m.p.=206 – 208ºC, M=386

Anal. calc. for $C_{16}H_{14}N_6O_4S$; C% 49.74; H% 3.62; N% 21.76; S% 8.29. Found: C% 49.88; H% 3.93; N% 21.96; S% 8.58.

IR (ν, cm^{-1}): 3108 (NH); 1627 (CO); 756 (CHAr); 1253 (C=S); 1347 (NO_2 sym.); 1541 (NO_2 asym.).

^{1}H-NMR (DMSO-d6, 400 MHz), δ (ppm): 3.29 (s, 3H, OCH_3); 6.88-6.91 (d, 2H, CHAr); 7.21-7.23 (d, 2H, CHAr); 7.74-7.77 (d, 1H, CHAr); 8.24-8.27 (d, 1H, CHAr); 8.40 (s, 1H, CHAr); 8.89 (s, 1H, CHAr); 9.59-9.62 (d, 2H, NH); 10.39 (s, 1H, NH).

Synthesis of 2-[(5'-nitro-1H-indazol-1'-yl)-carbonyl]-N-(p-bromophenyl)-hydrazincarbothioamide (VI)

White solid, yield 80%, m.p.=146 – 148ºC. M=435

Anal. calc. for $C_{15}H_{11}BrN_6O_3S$; C% 41.37; H% 2.52; Br% 18.36; N% 19.31; S% 7.35. Found: C% 41.52; H% 2.85; Br% 18.55; N% 19.53; S% 7.66.

IR (ν, cm^{-1}): 3049 (NH); 1622 (CO); 751 (CHAr); 1255 (C=S); 1352 (NO_2 sym.); 1539 (NO_2 asym.); 628 (C-Br).

^{1}H-NMR (DMSO-d6, 400 MHz), δ (ppm): 7.46-7.49 (d, 2H, CHAr); 7.59-7.62 (d, 2H, CHAr); 7.84-7.86 (d, 1H, CHAr); 8.28-8.30 (d, 1H, CHAr); 8.47 (s, 1H, CHAr); 8.83 (s, 1H, CHAr); 9.89-9.95 (d, 2H, NH); 10.60 (s, 1H, NH).

Synthesis of 2-[(5'-nitro-1H-indazol-1'-yl)-carbonyl]-N-(p-chlorophenyl)-hydrazincarbothioamide (VII)

White solid, yield 81%, m.p.=200 – 202ºC, M=391

Anal. calc. for $C_{15}H_{11}ClN_6O_3S$; C% 46.03; H% 2.81; Cl% 9.07; N% 21.48; S% 8.18. Found: C% 46.17; H% 3.11; Cl% 9.26; N% 21.72; S% 8.43.

IR (ν, cm^{-1}): 3127 (NH); 1628 (CO); 754 (CHAr); 1252 (C=S); 1341 (NO_2 sym.); 1530 (NO_2 asym.); 667, 727 (C-Cl).

^{1}H-NMR (DMSO-d6, 400 MHz), δ (ppm): 7.41-7.46 (m, 4H, CHAr); 7.70-7.73 (d, 1H, CHAr); 8.41 (s, 2H, CHAr); 8.54 (s, 1H, CHAr); 9.76-9.79 (d, 2H, NH); 10.49 (s, 1H, NH).

Synthesis of 2-[(5'-nitro-1H-indazol-1'-yl)-carbonyl]-N-(p-iodophenyl)-hydrazincarbothioamide (VIII)

White solid, yield 82%, m.p.=172 – 174ºC, M=482

Anal. calc. for $C_{15}H_{11}IN_6O_3S$; C% 37.34; H% 2.28; I% 26.32; N% 17.42; S% 6.63. Found: C% 37.53; H% 2.52; I% 26.65; N% 17.66; S% 6.87.

IR (ν, cm^{-1}): 3117 (NH); 1616 (CO); 1229 (C=S); 1333 (NO_2 sym.); 1519 (NO_2 asym.); 788 cm^{-1} disubstituted aromatic ring, 623 (C-I).

^{1}H-NMR (DMSO-d6, 400 MHz), δ (ppm): 7.39-7.41 (m, 4H, CHAr); 7.67-7.71 (d, 1H, CHAr); 8.37 (s, 2H, CHAr); 8.53 (s, 1H, CHAr); 9.78-9.81 (d, 2H, NH); 10.56 (s, 1H, NH).

4. Quantum - Mechanical Characterization of the Studied Compounds

HyperChem 8.06 molecular modeling software was used (based on quantum mechanics method PM3, parameteric method 3) (Stewart, 1989), with Polak-Ribiere optimization algorithm, restricted Hartree-Fock wavefunction, the convergence limit of 0.0001 kcal/mol and RMS gradient of 0.0001 kcal/(Å mol).

The structural optimized formula of 2-[(5'-nitro-1H-indazol-1'-il)-carbonyl]-N-phenylhydrazincarbothioamide (III) is represented in Fig. 2.

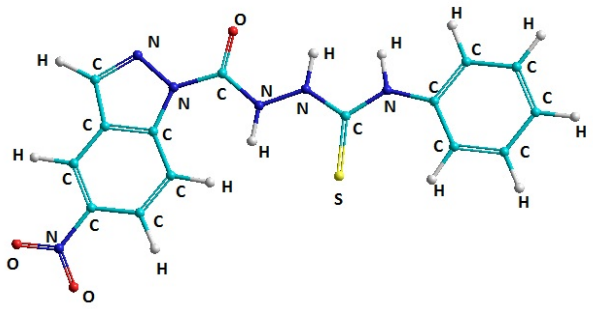

Fig. 2 – The structural optimized of compound III.

The structural optimized formula of 2-[(5'-nitro-1H-indazol-1'-yl)-carbonyl]-N-(p-tolyl)-hydrazincarbothioamide (IV) is represented in Fig. 3.

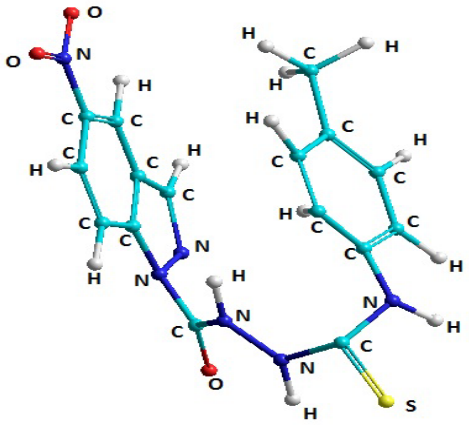

Fig. 3 – The structural optimized of compound IV.

The structural optimized formula of 2-[(5'-nitro-1H-indazol-1'-yl)-carbonyl]-N-(p-metoxiyphenyl)-hydrazincarbothioamide (V) is represented in Fig. 4.

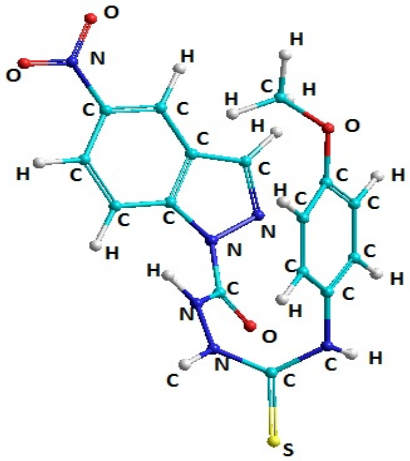

Fig. 4 – The structural optimized of compound V.

The structural optimized formula of 2-[(5'-nitro-1H-indazol-1'-yl)-carbonyl]-N-(p-bromophenyl)-hydrazincarbothioamide (VI) is represented in Fig. 5.

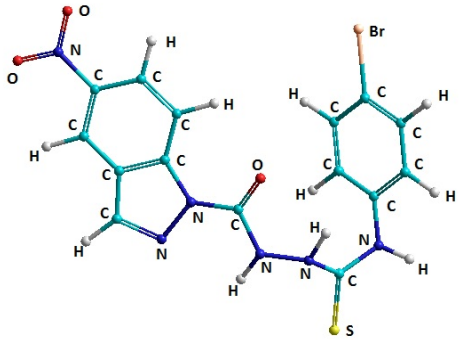

Fig. 5 – The structural optimized of compound VI.

The structural optimized formula of 2-[(5'-nitro-1H-indazol-1'-yl)-carbonyl]-N-(p-chlorophenyl)-hydrazincarbothioamide (VII) is represented in Fig. 6.

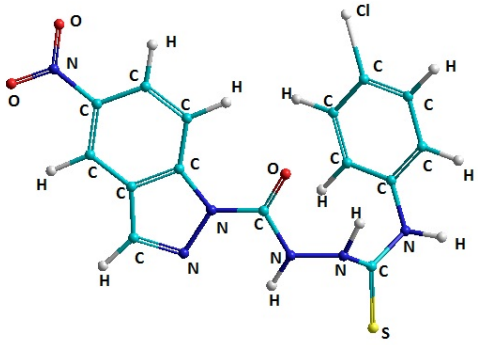

Fig. 6 – The structural optimized of compound VII.

The structural optimized formula of 2-[(5'-nitro-1H-indazol-1'-yl)-carbonyl]-N-(p-iodophenyl)-hydrazincarbothioamide (VIII) is represented in Fig. 7.

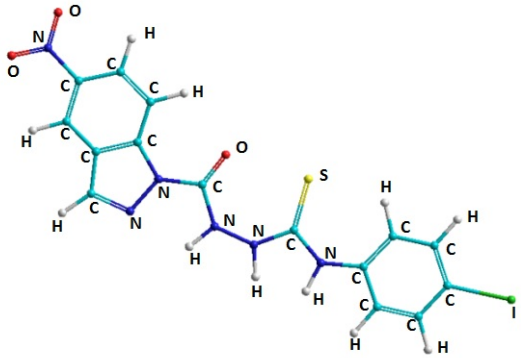

Fig. 7 – The structural optimized of compound VIII.

In Table 5 some of the most representative structural and energetic parameters are presented.

Table 5
Some Electro-Optical and Structural Propertiers for Molecules Studied

Properties	Molecule III	Molecule IV	Molecule V	Molecule VI	Molecule VII	Molecule VIII
Dipole moment [D]	6.73	5.82	3.82	3.07	2.94	9.72
Total energy [kcal/mol]	-92082.51	-95295.49	-102250.41	-99847.01	-98999.80	-98341.02
Binding energy [kcal/mol]	-3932.07	-3977.02	-4259.42	-3868.12	-3882.12	-3843.20
Heat of formation [kcal/mol]	179.59	409.72	186.88	218.17	206.42	241.87
Log P	-3.91	-3.76	-4.90	-3.86	-4.13	-3.39
Hydration energy [kcal/mol]	-18.79	-14.83	-17.08	-17.54	-17.50	-18.50
Refractivity [$Å^2$]	102.68	106.97	109.06	110.22	107.40	115.00
Polarizability [$Å^2$]	36.34	38.17	38.81	38.96	38.26	41.36
Mass [u. a.m]	356.36	370.39	386.38	435.25	390.80	482.26
Volume [$Å^3$]	912.84	881.85	911.11	949.06	925.51	983.69
Surface Area [$Å^2$]	549.90	496.63	516.35	553.64	540.59	588.29
E_{HOMO} [eV]	-9.06	-9.27	-8.85	-9.18	-9.19	-8.35
E_{LUMO} [eV]	-1.56	-2.43	-1.89	-2.02	-2.06	-1.49
$\Delta E=\lvert E_{HOMO}-E_{LUMO}\rvert$ [eV]	10.62	11.69	10.74	11.19	11.25	9.83

The difference $E_{HOMO} - E_{LUMO}$ represents the lowest energy electronic excitation that is possible in a molecule.

$$\Delta E = |E_{HOMO} - E_{LUMO}| \quad (9)$$

The QSAR (Quantitative Structure – Activity Relationships) parameters (Gallegos, 2004) correlate the molecular structure or the properties derived from molecular structure with a particular kind of chemical or biochemical activity.

LogP (Parthasarathi *et al*., 2012) is related to the hydrophobic character of the molecule, which plays an important role in biochemical interactions. A negative value of log P indicates the hydrophilicity, for the studied compounds, that plays an important role in biochemical interactions.

5. Toxicity of New Compounds

The synthesized compounds were tested for their toxicity degree and their lethal dose (LD_{50}) was determined. The toxicological data obtained (Table 6) confirm that 2-[(5'-nitro-1H-indazol-1'-yl)-carbonyl]-N-arilhydrazin-carbothioamide (thiosemicarbazides) (III - VIII) have low toxicity, which recommends them for further biological tests.

Table 6
The LD_{50} Values of the Tested Compounds

Compound	Administration route	Test animals	LD_{50} [mg/kilobody]
III	i.p.	mice	8443
IV	i.p.	mice	9223
V	i.p.	mice	9621
VI	i.p.	mice	9201
VII	i.p.	mice	8922
VIII	i.p.	mice	9274

Toxicity was estimated through intraperitoneal administration of the substances under analysis, as suspensions, in Tween 80, on groups formed of 14 mice each 20±5 g, according to the Kärber method (Hamilton *et al*., 1978). The animals tested were followed, their mortality being recorded at intervals of 7 days.

6. Conclusions

The ethyl ester of the ethyl ester of 5-nitroindazol-1-yl-formic acid and the 5-nitroindazol-formic hydrazide were prepared.

The optimal conditions in which, six new thiosemicarbazides (III – VIII) were synthesized by the reaction of hydrazide with different isothiocyanates.

The structure of the compounds III – VIII was confirmed through elemental and spectral (FT-IR and 1H-NMR) analyses.

The structural features of new thiosemicarbazides III-VIII and their QSAR parameters were established using HyperChem 8.06.

The toxicity of the new thiosemicarbazides was established and the lethal dose (LD_{50}) was determined.

Acknowledgements. This work was financially supported by the Internal research grant of University of Medicine and Pharmacy "Grigore T. Popa" Iași Nr. 30878/30.12.2014.

REFERENCES

Azzouz A., Leontie M., Dorohoi D.O., Gheorghies C., *Elemente de strategie în design industrial*, Edit. Plumb, Bacău, 1998.

Berhe S., Slupe A., Luster C., Chartier H., Warner D., Zalkow L., Burgess E., Enwerem N., Bakare O., *Synthesis of 3-[(N-Carboalkoxy)Ethylamino]-Indazole-Dione Derivatives and their Biological Activities on Human Liver Carbonyl Reductase*, Bioorg. Med. Chem., **18**, 134 (2010).

Bhat A.R., Athar F., Azam A., *Bis-Pyrazolines: Synthesis, Characterization and Antiamoebic Activity as Inhibitors of Growth of Entamoeba Histolytica*, Eur. J. Med. Chem., **44**, 426 (2009).

Bukovski L., Janowiec M., Zwolska Z., Andrezejezyk Z., *Some Reactions of 2-Cyanomethylimidazo[4,5-b]Pyridine with Isothiocyanates. Antituberculotic Activity of the Obtained Compounds*, Pharmazie, **53**, 373-376 (1998).

Cheptea C., Șunel V., Profire L., Popa M., Lionte C., *New Hydrazones of 5-Nitroindazol-1-yl-Acethydrazide with Pharmacological Potential*, Bul. Inst. Polit. Iași, sIIc., **55 (59)**, 87 (2009).

Cigu T.A., Nechifor C.D., Șunel V., Dorohoi D.O., Cheptea C., *Optimization Reaction for Obtaining New Hydrazidones with Biological Action*, Rev. Roum. Chim., **59,** *9*, 739 (2014).

Cheptea C., Șunel V., Stan C., Dorohoi D.O., *New Derivatives of 5-Nitro-Indazole with Potential Antitumor Activity*, Revue Roumaine de Chimie, **57**, 229 (2012).

El-Asmy A., Al-Gammal O., Saad D., Ghazy S., *Synthesis, Characterization, Molecular Modeling and Eukaryotic DNA Degradation of 1-(3,4-Dihydroxybenzylidene)Thiosemicarbazide Complexes*, J. Mol. Struct., **934**, 9-22 (2009).

Fahmy H., *Synthesis of Some New Triazoles as Potential Antifungal Agents*, Bull. Chim. Farmac., **140**, *6*, 422-427 (2001).

Fisher L., *Design for Environment, Creating Eco-Efficient Products and Processes*, Ed. Mc. Graw Hill, New York, 1996.

Gallegos S.A., *Molecular Quantum Similarities in QSAR: Applications in Computer – Aided Molecular Design*, PhD Thesis, Universitat de Girona, 2004.

Hamilton M.A., Russo R.C., Thurston R.V., *Trimmed Spearman-Karber Method for Estimating Median Lethal Concentrations in Bioassays*, Environ. Sci, Technol., **12**, *4*, 417 (1978).

Huang L., Shih M.L., Chen S.H., Pan L.S., Teng M.C., Lee F., Kuo S., *Synthesis of N^2-(Substituted Benzyl)-3-(4-Methylphenyl)Indazoles as Novel Anti-Angiogenic Agents*, Bioorg. Med. Chem., **14**, 528 (2006).

Hurjui I., Cheptea C., Dascălu C.F., Hurjui L., Peptu C., Șunel V., Dorohoi D.O., *Optimization Reaction of Some 1, 4-Disubstituted Thiosemicarbazides with Tuberculostatic Activity*, Dig. J. Nanomater Bio., **7**, 1747 (2012).

Liesen A., Aquino T., Carvalho C., Lima V., Aranjo J., Lima J., Faria A., Melo E., Alves A., Alves E., *Synthesis and Evaluation of anti-Toxoplasma Gondii and Antimicrobial Activities of Thiosemicarbazides, 4-Thiazolidinones and 1,3,4-Thiadiazoles*, Eur. J. Med. Chem., **45**, 3685 (2010).

Moise M., Șunel V., Profire L., Popa M., Desbrieres J., Peptu C., *Synthesis and Biological Activity of Some New 1,3,4-Thiadiazole and 1,2,4-Triazole Compounds Containing a Phenylalanine Moiety*, Molecules, **14**, *7*, 2621-2631 (2009).

Moise M., Șunel V., Dulcescu M.M., Dorohoi D.O., *Mathematic Modelling to Optimize the Obtaining Process of New Thiosemicarbazides Derived from N-(P-Nitrobenzoyl)-D,L-Phenylalanine*, Rev. de Chimie (București), **61**, 229 (2010).

Parthasarathi R., Subramanian V., Roy D.R., Chattaraj P.K., Bioorganic & Medicinal Chemistry, *In Advanced Methods and Applications in Chemoinformatics: Research Progress and New Applications*, E.A. Castro, A.K. Haghi (Eds.), 2012.

Plech T., Wujec M., Siwec A., Kosikowska U., Malm A., *Synthesis and Antimicrobial Activity of Thiosemicarbazides,* S-*Triazoles and their Mannich Bases Bearing 3-Chlorophenyl Moiety*, Eur. J. Med. Chem., **46**, 241 (2011).

Ribeira M., Cabral J., Cimas A., *Experimental and computational study of the energetics of 5- and 6-aminoindazole*, J. Chem. Thermodynamics, **42**, 1240 (2010).

Rodriguez J., Gerpe A., Aguirre G., Kemmerling U., Piro O., Aran V., Maya J., Azar C.O., Gonzalez M., Cerecetto H., *Study of 5-Nitroindazoles' anti-Trypanosoma Cruzi Mode of Action: Electrochemical Behaviour and ESR Spectroscopic Studies*, Eur. J. Med. Chem., **44**, 1545 (2009).

Seleeman H.S., El-Shetary B.A., Khalil S., Mostafa M., Shebl M., *Structural Diversity in Copper(II) Complexes of bis(Thiosemicarbazone) and bis(Semicarbazone) Ligands*, J. Coord. Chem., **58**, 479-493 (2005).

Shelke S., Mhaske G., Gadakh S., Gill C., *Green Synthesis and Biological Evaluation of Some Novel Azoles as Antimicrobial Agents*, Bioorg. Med. Chem. Lett., **20**, 7200 (2010).

Stewart J.J.P., *Optimization of Parameters for Semi-Empirical Methods I-Metho*, Computational Chemistry, **10**, *2*, 209 (1989).

Ulusoy N., *Synthesis and Antituberculosis Activity of Cycloalkylidenehydrazide and 4-Aza-1-Thiaspiro[4.5]Decan-3-one Derivatives of Imidazo[2,1-b]Thiazole*, Arzneim-Forsch. Drug. Res., **52**, *7*, 565-571 (2002).

Yakaiah T., Ligaiah V.P., Naraiah B., Shireesha B., Kumar B., Gururaj S., Parthasarathy T., Sridhar B., *Synthesis and Structure–Activity Relationships of Novel Pyrimido[1,2-b]Indazoles as Potential Anticancer Agents Against A-549 Cell Lines*, Bioorg. Med. Chem. Lett., **17**, 3445 (2007).

www.hyper.com (HyperChem, Molecular Visualisation and Simulation Program Package, Hypercube, Gainsville, Fl, 32601).

OPTIMIZAREA REACȚIILOR DE SINTEZĂ ALE UNOR NOI TIOSEMICARBAZIDE PROVENITE DIN 5-NITROINDAZOL

(Rezumat)

Noi tiosemicarbazide cu activitate biologică, derivate din 5-nitroindazol, au fost sintetizate. Pentru a obține tiosemicarbazidele, formil hidrazida 5-nitroindazol-1-yl

se tratează cu diferiți izotiocianați aromatici. Au fost stabilite condițiile în care reacțiile au loc cu cel mai mare randament. Reacțiile de optimizare au fost realizate într-un experiment factorial de tip 3^2. Unele proprietăți fizico-chimice ale noilor compuși sintetizați au fost stabilite teoretic prin utilizarea HyperChem 8.6.0. Structura chimică a noilor compuși sintetizați a fost confirmată prin analiză elementară și spectrală (FT-IR, 1H-RMN). Noii compuși au fost testați din punct de vedere al toxicității.

BULETINUL INSTITUTULUI POLITEHNIC DIN IAŞI
Publicat de
Universitatea Tehnică „Gheorghe Asachi” din Iaşi
Volumul 63 (67), Numărul 1, 2017
Secţia
MATEMATICĂ. MECANICĂ TEORETICĂ. FIZICĂ

STATISTICAL STUDY OF IMPACT OF THE USE OF COMPUTER SIMULATIONS ON THE IMPROVEMENT OF STUDENTS' MARKS

BY

MARIUS-MIHAI CAZACU[1,*], GABRIELA COVATARIU[2] and IRINA RADINSCHI[1]

"Gheorghe Asachi" Technical University of Iași,
[1]Department of Physics
[2]Department of Structural Mechanics

Received: January 30, 2017
Accepted for publication: March 7, 2017

Abstract. Since 2008 we have designed various computer simulations of physics phenomena which are addressed to first year students at the Faculty of Civil Engineering and Building Services. The main purpose is to improve students' understanding of physics phenomena and their ability to do the practical laboratory work. In the last decade, we have carried out computer simulations of physics phenomena with the aid of programs and technologies like Adobe Flash, HTML5 and JavaScript. We emphasize significant progress in our students' skills of work in both real physics laboratory and Virtual Physics Laboratory (VPL), and in the increase of their marks at the laboratory tests and in final exams. The present paper is focused on a statistical survey that we have performed to establish the improvement of our students' marks in the last three academic years. Further, an additional statistical study of the use of computer simulations and Virtual Physics Laboratory (VPL) has been elaborated.

Keywords: statistical study; computer simulations; physics phenomena; Adobe Flash; HTML5; JavaScript.

[*]Corresponding author; *e-mail*: marius.cazacu@tuiasi.ro

1. Introduction

In recent years, motivated by the requirement of improving the teaching and learning processes we have designed computer simulations of various physics phenomena. Computer simulations are important learning tools in Civil Engineering and offer many opportunities of easy understanding of different physics phenomena and laws. One of the most important tasks at the physics laboratory is the improvement of students' marks at the laboratory tests. The activity in the real physics laboratory is certainly better accomplished by the use of computer simulations. For faster communication with our students computer simulations are placed on the Internet in the Virtual Physics Laboratory (VPL).

Internationally, many researchers carried out computer simulations which helped students to better understand the laboratory works and the curricula objectives (www.phet.colorado.edu; http://wildcat.phys.northwestern.edu; www.myphysicslab.com; http://virlab.virginia.edu; Gould *et al.*, 2007; Jong *et al*., 2013; Uribe *et al*., 2016). In the last decade, we have focused our efforts on the development of computer simulations of physics phenomena (Radinschi *et al*., 2008a; Radinschi *et al*., 2008b; Radinschi *et al*., 2015; Radinschi *et al*., 2016) elaborated in Adobe Flash (http://adobe.com/products/flash), HTML5 (https://developer.mozilla.org/en-US/docs/Web/Guide/HTML/HTML5) and JavaScript (https://www.javascript.com/). Computer simulations are useful tools that reproduce in a realistic way the real devices and facilitate our teacher-leader roles. The implementation of different computer simulations in our physics laboratory had a high impact on the learning process, and also led to a considerable improvement of students' marks.

Further, our first year students have shown a high interest in the use of computer simulations. They accessed the Virtual Physics Laboratory (VPL) from the physics laboratory and also from home and campus. We point out that most of the students have preferred to work both in the real physics laboratory and in the Virtual Physics Laboratory (VPL). It is worth to mention that almost none of the students have chosen to work only in the Virtual Physics Laboratory (VPL). As a result of the connection between the laboratory activities and the use of the Virtual Physics Laboratory (VPL) the students' scores at the laboratory tests and in final exams have significantly increased.

The present paper is organized as follow. In section 2 we perform a brief presentation of the Virtual Physics Laboratory (VPL). Section 3 is devoted to the development of a statistical study of the impact of the use of computer simulations on the improvement of students' marks at the laboratory tests and in final exams in the last three academic years. Further, a statistical study concerning the use of computer simulations and of the Virtual Physics Laboratory (VPL) is presented. Section 4 is assigned to discussion and concluding remarks.

2. Description of the Virtual Physics Laboratory (VPL)

Our computer simulations of physics phenomena developed in Adobe Flash, HTML5 and JavaScript are posted in the Virtual Physics Laboratory (VPL) at the web address http://server.ce.tuiasi.ro/~radinschi/simulation/default.html. Since 2008 to present, our interest in developing computer simulations of physics phenomena has considerably increased. Our first computer simulations were elaborated with the aid of Adobe Flash. As examples, we present in Fig. 1 and Fig. 2 the screenshots of the computer simulations developed for the study of the laws of the photoelectric effect.

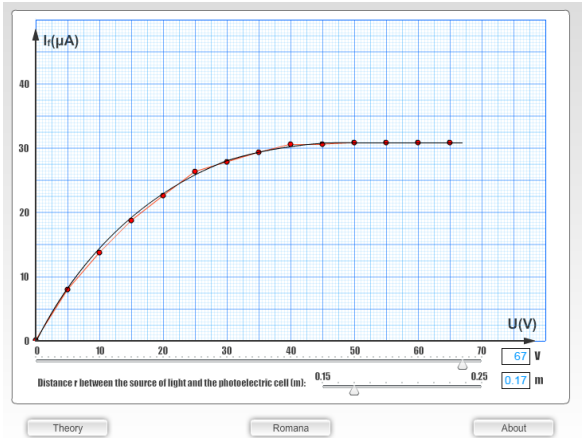

Fig. 1 – Study of the laws of the photoelectric effect, increase of the current up to saturation.

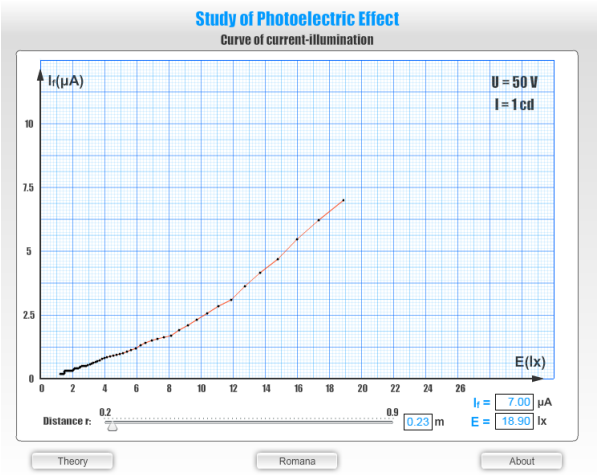

Fig. 2 – Study of the laws of the photoelectric effect, the current-illumination curves.

Fig. 3 shows the screenshot of the computer simulation carried out for the study of two perpendicular harmonic oscillations of the same frequency. This computer simulation has been developed in 2015 with the aid of the HTML5 and JavaScript technologies.

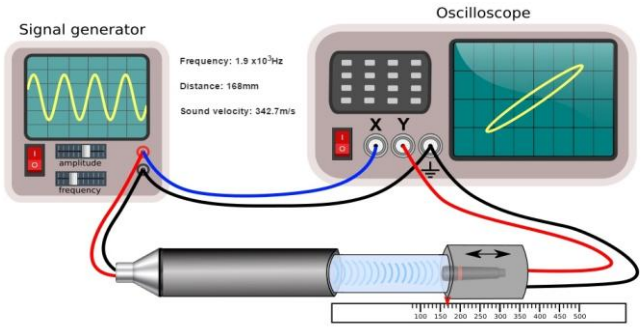

Fig. 3 – Study of two perpendicular harmonic oscillations of the same frequency.

3. Statistical Study of the Impact of the Use of Computer Simulations

We have performed a statistical study designated to establish the improvement of our students' marks in the last three academic years both at the laboratory tests and in final exams. We have focused our research on the results obtained by our first year students who study in Romanian (RO), and in English (EN), respectively. Further, we have also performed the statistical study for both series of students (RO) + (EN).

In Fig. 4 we present the relative frequencies of the marks in final exams for the two series of students (EN) – left panel, (RO) – middle, and in general (RO) + (EN) – right panel. The comparison is made for the last three academic years.

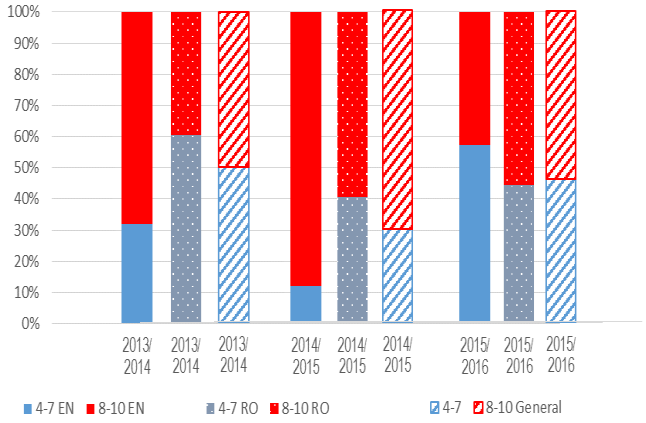

Fig. 4 – The relative frequencies of the marks for the two series of students (EN) and (RO), and in general (RO) + (EN).

The comparison for the last three academic years for the marks at the laboratory tests is presented in Fig. 5 in form of relative frequencies of the marks in general (RO) + (EN), and for the two series of students (RO) and (EN).

By comparing students' marks at the laboratory tests, we notice a permanent increase in the percentage of high scores (8-10). Thus, we have an increase of 36.88% in the case of the laboratories held in English, 26.55% for the laboratories in Romanian, leading to an overall increase of 29.68% between the academic years of study 2013-2014 and 2015-2016.

In Fig. 6 we present the maps of marks obtained at the laboratory tests by the first year students (RO) + (EN) in the last three academic years. These students have used the computer simulations. From this statistical study we conclude that there is a significant increase in the marks of the students. This increase is also due to the use of the Virtual Physics Laboratory (VPL).

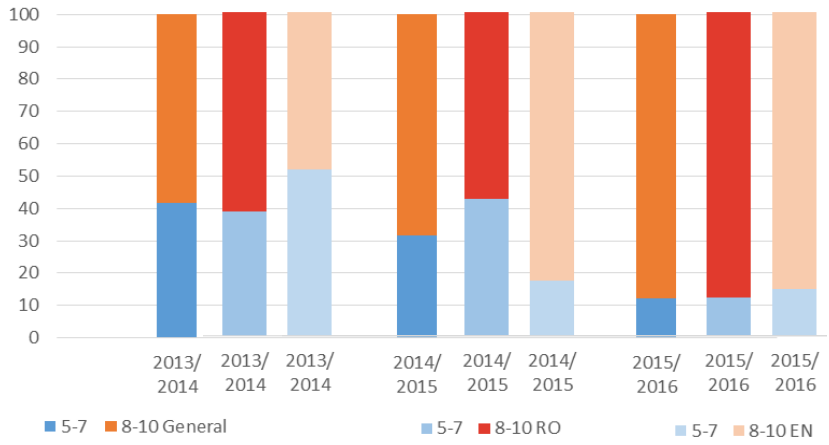

Fig. 5 – The relative frequencies of the marks at the laboratory tests in general (RO) + (EN), and for the two series of students (RO) and (EN).

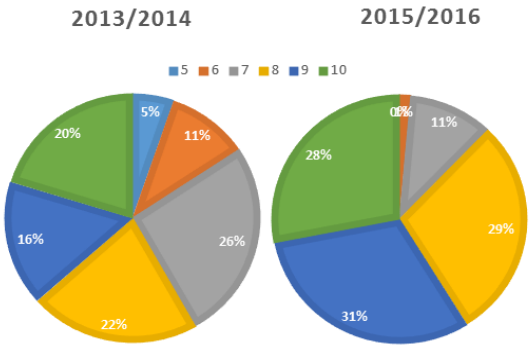

Fig. 6 – The comparison between the maps of marks at the laboratory tests in the academic years 2013/2014 and 2015/2016, respectively.

In Fig. 7 we show the increase of the number of students who used to work in the Virtual Physics Laboratory (VPL). We estimated this increase this academic year by comparison with the academic year 2013-2014.

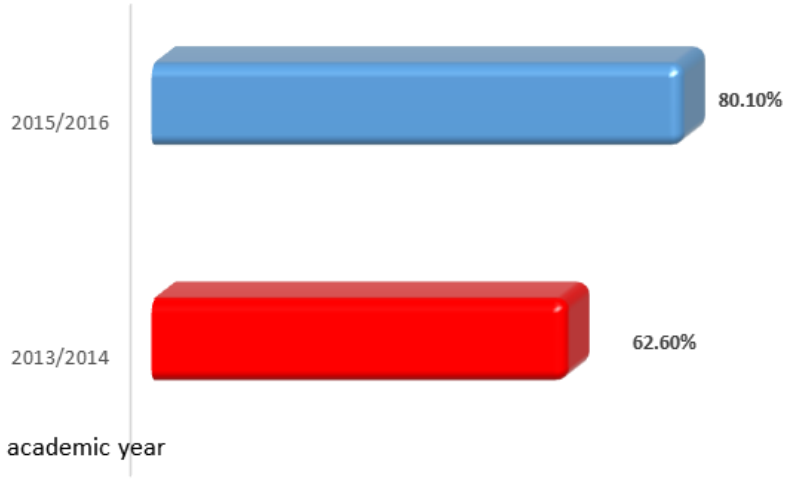

Fig. 7 – Comparison of the students who used the Virtual Physics Laboratory (VPL) [%].

It is worth to mention, that the development of our Virtual Physics Laboratory (VPL) has led to an additional increase of 17.5 % in the number of students who used the computer simulations. We notice an increase of the marks at the laboratory tests and in final exams for the students who have worked with computer simulations and the Virtual Physics Laboratory (VPL).

3. Discussion and Concluding Remarks

Considering the growing interest of our students' community in the study of physical phenomena with the aid of computer simulations we have developed new applications by using HTML5 and JavaScript technologies, and better organized the Virtual Physics Laboratory (VPL).

In this paper we present a statistical study performed to establish the improvement of our first year students' marks in the last three academic years. The statistical study comprises two parts. First, we have the statistics of the marks in final exams in the last three academic years. Second, we present the statistics of the marks at the laboratory tests. This statistical study has been performed for the academic years 2013-2014, 2014-2015 and 2015-2016, respectively. In addition, we present the increase of the number of students who used to work in the Virtual Physics Laboratory (VPL) in the last three academic years.

From our statistical study it results that the use of computer simulations and Virtual Physics Laboratory (VPL) help our students to improve their learning skills and get higher marks at the laboratory tests and in final exams. Further, together with the traditional work in the physics laboratory the computer simulations are useful tools to study physics phenomena and laws, and for learning physics.

From Fig. 4 it results an improvement of the marks of our students in final exams in the last three academic years.

Concerning the marks at the laboratory tests, from Fig. 5 we conclude that there is a significant improvement in the last three academic years of the percentage of high marks for the students who study in Romanian (RO), in English (EN) and in general (RO) + (EN), respectively.

Fig. 6 presents the comparison between the maps of marks at the laboratory tests in the academic years 2013/2014 and 2015/2016 in general (RO) + (EN), respectively. The increases in the percentage of marks are of 7% for 8 mark, 15% for 9 mark and 8% for 10 marks.

REFERENCES

Gould H., Tobochnik J., Christian W., *An Introduction to Computer Simulations Methods: Applications to Physical Systems*, 3rd. Ed., Addison-Wesley, 2007.

Jong T., Linn M.C., Zacharia Z.C., *Physical and Virtual Laboratories in Science and Engineering Education*, Science, **340**, *6130*, 305-308 (2013).

Uribe M.R., Magana A.J., Bahk J.H., Shakouri A., *Computational Simulations as Virtual Laboratories for Online Engineering Education: A Case Study in the Field of Thermoelectricity*, Comput. Appl. Eng. Educ., **24**, *3*, 428-442 (2016).

Radinschi I., Damoc C., Cehan A., Cehan V., *Computer Simulations of Physics Phenomena Using Flash*, Proc. of the 5th International Conference on Hands-on Science Formal and Informal Science Education, HSCI 2008, Espaço Ciência, Olinda-Recife, Brasil, 147-152 (2008).

Radinschi I., Damoc C., *Computer Simulations for Physics Laboratory*, Proc. of the Sixth International Symposium „Computational Civil Engineering 2008", CCE 2008, 441-447 (2008).

Radinschi I., Covatariu G., Cazacu M.M., *Maple Program for Studying Physics Phenomena with Applications in Civil Engineering*, Proceedings of International Symposium Computational Civil engineering CCE 2015, 29 May 2015, Iaşi, 279-290 (2015).

Radinschi I., Fratiman V., Cazacu M.M., Covatariu G., *A Computer Aided Study of Two Perpendicular Harmonic Oscillations of the Same Frequency*, Bul. Inst. Polit. Iași, Section Mathematics. Theoretical Mechanics, Physics, **62 (66)**, *1*, 55-66 (2016).

http://adobe.com/products/flash

https://developer.mozilla.org/en-US/docs/Web/Guide/HTML/HTML5

http://phet.colorado.edu

http://virlab.virginia.edu

http://wildcat.phys.northwestern.edu
www.javascript.com/
www.myphysicslab.com,

STUDIU STATISTIC PRIVIND IMPACTUL UTILIZĂRII SIMULĂRII COMPUTAȚIONALE LA ÎMBUNĂTĂȚIREA NOTELOR STUDENȚILOR

(Rezumat)

Începând cu anul 2008, am conceput diverse simulări pe calculator ale fenomenelor fizice adresate studenților de la Facultatea de Construcții și Instalații. Scopul principal este de a îmbunătăți atât înțelegerea de către studenți a fenomenelor fizicii cât și de dezvoltare a abilităților practice. În ultimul deceniu, am realizat simulări pe calculator ale fenomenelor fizicii cu ajutorul programelor și tehnologiilor precum Adobe Flash, HTML5 și JavaScript. Am observat progresul semnificativ a aptitudinilor studenților noștri de a lucra atât în laboratorul real de fizică, cât și în laboratorul virtual de fizică (VPL) și mai mult am observat creșterea notelor la testele de laborator și la examenele finale. Lucrarea de față se concentrează pe un studiu statistic pe care l-am efectuat pentru a stabili îmbunătățirea notelor studenților noștri din ultimii trei ani universitari. În plus, a fost elaborat un studiu statistic suplimentar privind utilizarea simulărilor pe calculator și a laboratorului virtual de fizică (VPL).

BULETINUL INSTITUTULUI POLITEHNIC DIN IAŞI
Publicat de
Universitatea Tehnică „Gheorghe Asachi” din Iaşi
Volumul 63 (67), Numărul 1, 2017
Secţia
MATEMATICĂ. MECANICĂ TEORETICĂ. FIZICĂ

CHOLESTERIC LIQUID CRYSTALS AND THEIR APPLICATIONS IN TEMPERATURE MEASUREMENTS AND IN CONTAMINATION DETECTION

BY

NICOLETA MELNICIUC PUICĂ[1], ANA MARIA CIUBARA[2], MAGDALENA POSTOLACHE[3] and DANA ORTANSA DOROHOI[4,*]

[1]”Alexandru Ioan Cuza” University of Iași,
Faculty of Orthodox Theology
[2]“Dunărea de Jos” University of Galați,
Faculty of Medicine and Pharmacy
[3]“B. P. Hașdeu” School Iași
[4]“Alexandru Ioan Cuza” University of Iași,
Faculty of Physics

Received: February 20, 2017
Accepted for publication: March 24, 2017

Abstract. Cholesteric liquid crystals form thin films with special optical properties. Their sensibility to the changes in temperature offers the means for measuring very small variations of local temperature and for evidencing the different mechanic and electromagnetic waves, by their thermal effects. Small amounts of contaminants can be detected in the atmosphere with devices containing cholesteric liquid crystalline layers due to the high sensitivity of their pitch to impurities. An experimental study in which small amounts of tetrahydrofuran vapors of tetrahydrofuran are evidenced by cholesteric layer embedded in polystyrene is realized in this paper.

Keywords: Cholesteric liquid crystals; chiral biphenyl; tetrahydrofuran; temperature determination; contaminant vaporous detection.

[*]Corresponding author; *e-mail*: ddorohoi@uaic.ro

1. Introduction

Liquid crystals are groups of substances named mesogens, with the mobility of fluids and the symmetry of inorganic crystals (Brown *et al*., 1971; De Gennes, 1974; Collings, 1977; Demus *et al*., 1998).

Discovered by Reinitzer (1888) in his study of the cholesterol salts, the new substances were denominated as "liquid crystals" by Liehmann (1889) to underline their double nature.

Liquid crystals can be classified in:

– thermotropic (their degree of order is essentially influenced by temperature);

– lyotropic (they are obtained from mixtures at a given concentration of amphiphilic molecules in a thermodynamically bad solvent for this type of molecules).

After about one hundred years from their discovery, liquid crystals became omnipresent in our life, in technics, in imagistics.

The great importance of both lyotropic and cholesteric liquid crystals in vital processes represent only a part from their large area of applications.

Some applications of cholesteric liquid crystals will be described in this paper, based on their physical and chemical properties.

Cholesteric liquid crystals are included in the group of thermotropic liquid crystals. They have the orientational order of achiral nematics, but the director is constrained in a layer–like structure to precess around the helical axis (HA) perpendicular on the director (Pershan, 1978; Muscutariu, 1981; Collings, 1997). Each layer (Fig. 1) composing Cholesteric contains molecules in a constant thermal agitation having preferential orientation given by the director versor ($\vec{n}$). The director configuration is helical and the repeated length is known as the pitch (p) of the cholesteric liquid crystal.

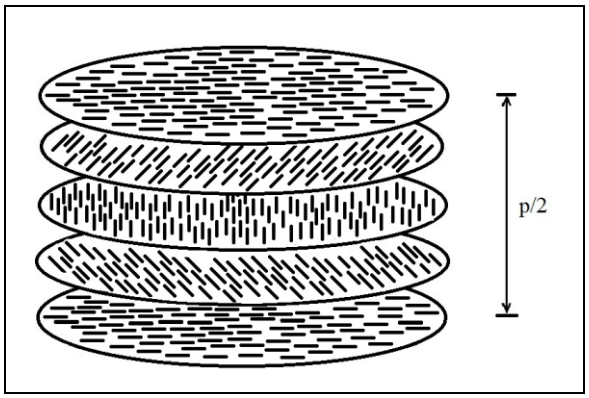

Fig. 1 – Orientation of the mesogenic molecules in a Cholesteric liquid crystal; Pitch (p) of cholesteric.

The mesogenic components of cholesteric liquid crystals (monomers, dimers, polymers) are intrinsically chiral or chiral dopant are added to non-chiral Nematics.

The cholesteric texture possesses a number of properties giving rise to the unique optical effects, such as:

– it is anisotropic uniax with negative birefringence;

– it is optically active with rotatory power many times higher that a normal optically active material;

– it is usually circularly dichroic as it can affect both right and left circularly polarized components of light;

– it scatters the incident white light in a similar manner as the solid crystals.

The ordered state of cholesteric liquid crystal is mainly determined by surface anchoring, cell thickness and also by applied fields (Moțoc and Muscutariu, 1986).

The cholesteric liquid crystals can change their pitch under external factors (changes in temperature or in pressure, variations in external fields). Consequently, they can display the changes in the external factors by changing their color (Meier *et al*., 1975; Kleinert and Maki, 1981; Bunning *et al*., 1996; Shibaev *et al*., 2015).

2. Structural Features of the Cholesteric Liquid Crystals

Observed with a polarizing microscope, cholesteric liquid crystal layers have different visual aspects (named textures) depending on their molecular chemical structure, on the orientation of the mesogen molecules related to the internal walls of the cell (in which liquid crystals are kept), or on the type of interactions between the mesogens and the anchoring molecules.

The molecules of cholesteric liquid crystals can adopt different orientations (Fig. 2) in the cells where they are kept (Muscutariu, 1981):

– Planar (homeotropic) orientation

– Homeotropic orientation

– Inclined orientation

The cells can have parallel or inclined walls (Fig. 2).

The relative orientation of the director versor ($\vec{n}$) and of the helical axis (HA) is suggested and also the angle θ between the director versor ($\vec{n}$) and the contact surface is plotted for the inclined walls of the cell, in Fig. 2.

In order to orient the mesogenic molecules in the vicinity of the cell surface, an adequate treatment of the contact surfaces (internal walls of the cell) is necessary. The known procedures (Dumitrașcu and Dorohoi, 2015) for this treatment can be classified in two main groups:

– mechanical treatment;

– chemical treatment.

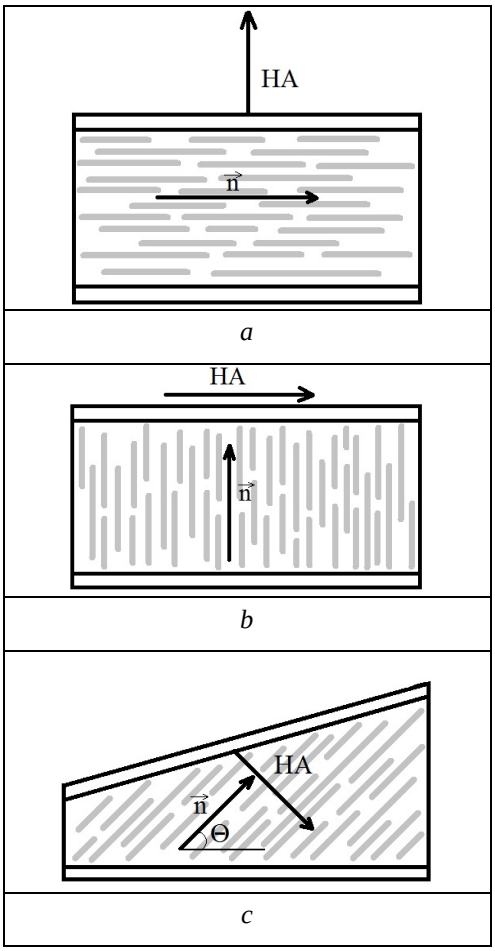

Fig. 2 – Orientation of the director versor ($\vec{n}$) and of the helical axis (HA) relative to the contact surface; *a* – Planar (homotropic) orientation ($\theta = 0$); *b* – Homeotropic orientation ($\theta = 90^o$); *c* – Inclined orientation ($0^o < 0 < 90^o$).

The orienting action of the internal surfaces of the cell in which cholesteric liquid crystal will be kept can be realized by chemical cleaning and treatment, by deposing of thin films of organic or inorganic materials on the internal surfaces, or by scratching or deformation of the surfaces.

In the case of non- scratched plane surfaces of the cells, the orientation procedure is based on intermolecular interactions or on the mechanical interactions with surface resulting from the anisotropy of the mesogen molecules.

In order to understand the functioning of the devices based on cholesteric liquid crystals one can have in mind that the mesogens are dipolar molecules or can become dipolar in interactions with external fields.

In the case of a planar homotropic anchoring, the director versor ($\vec{n}$) of the cholesteric is parallel to the surface of cell walls and the helical axis is perpendicular on the cell walls (Fig. 2*a*). The homeotropic cholesteric structure corresponds to a director versor perpendicular to the cell walls and the helical axis parallel to the cell walls (Fig. 2*b*).

The cells with plane but non- parallel opposite walls are used to visualize the irregularities in the homogeneous structures of cholesteric liquid crystal formed parallel to the edge of the cell, by the modifications in interference fringes obtained in monochromatic radiation, due to the periodic structure of the layer (Muscutariu, 1981).

The homogenous planar structure of a cholesteric is characterized by uniform texture, having a color that depends on the pitch of the helix and/or on the phase delay during the propagation through the liquid crystal. Various irregularities in the homogenous planar structures of cholesteric liquid crystals (defects in the networks) can be visualized at the polarizing microscope illuminated by white light, or by using a confocal microscope equipped for fluorescence (Dumitrașcu and Dorohoi, 2015).

3. Action of the Low Intensity Electric Fields on the Cholesteric Liquid Crystalline Layers

In the presence of low intensity electric fields, cholesteric liquid crystals can modify their structure.

Let us suppose that an external electric field of low intensity is applied perpendicularly on the walls of the special cell keeping the cholesteric liquid crystal in a planar orientation.

As a result of interaction between mesogen molecules and electric field rotational moments act on the mesogen molecules, tending to reorient them along the field lines, but the process is limited near the separation surfaces (Demus and Lothar, 1978).

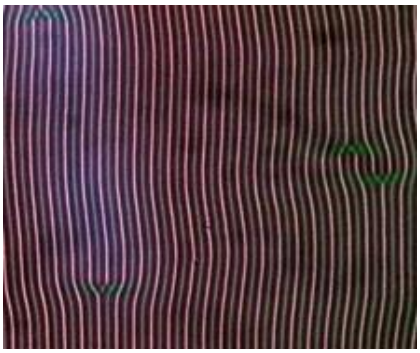

Fig. 3 – One dimensional undulations in p-azolyanisole for $d/p \leq 3$.

So, under the electric field action, the planar orientation of cholesteric liquid crystals can be modified by periodical sinusoidal distortions called undulations (Dumitrașcu and Dorohoi, 2015). The dependence of the undulation aspects on the ratio d/p (thickness of the cholesteric liquid crystals layer/ pitch) is illustrated in Figs. 3 and 4.

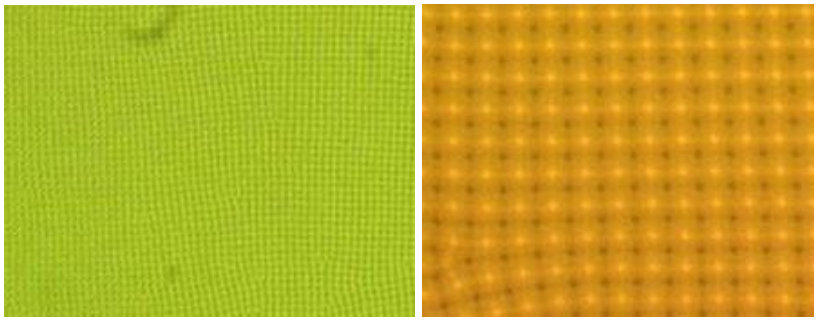

Fig. 4 – Bidimensional undulations in Cholesteric liquid crystals for d/p > 10 (The size of the pitch increases from left to right).

Weak electric fields applied to cholesteric liquid crystals produce undulations significantly depending on the ratio between the layer thickness and the pitch of helical structure. Using a polarizing microscope unidirectional undulations were observed (Fig. 3) for $d/p \leq 3$ and bidirectional undulations for $d/p > 10$ (Fig. 4).

The spatial period of the undulations depends on the thickness of the cell and the cholesteric pitch.

The bidimensional undulations in cholesteric liquid crystals produce diffraction of the laser beams. So, the undulation phenomenon can be used in determining the spatial period of undulations and the pitch, when the cell thickness is known.

The homeotropic cholesteric liquid crystals have the director versor oriented perpendicularly on the cell walls and the helix axis parallel to the walls surface. The structures obtained in very weak electric fields are named "digital print" textures. The aspects of such textures depends on the ratio d/p (thickness of the cell/ pitch of cholesteric) and on the strength of the anchoring to the cell surfaces. For strong anchoring of the mesogene molecules to the cell surfaces, the rotation of the director versor around the helix axis is totally lost. The effect has been evidenced for very thin liquid crystal layers.

Based on the important property of cholesteric liquid crystals to change their pitch under external influence (changes in temperature, pressure, in the presence of some mechanical waves (ultrasounds) or electromagnetic waves (infrared, microwave), a great number of their applications were developed.

4. Contaminant Vapors Action on the Cholesteric Liquid Crystalline Layers

Based on the sensing approach for the polar solvent vaporous, some applications of cholesteric liquid crystals were developed for monitoring the solvent vapor concentrations (Mujahid *et al*., 2010; Shibaev *et al.*, 2015).

A special cell with lateral transparent windows contains in vertical position one Cholesteric liquid crystal (a mixture of chiral biphenyls achieved from Merck Company) embedded in a thin polyurethane layer. A jet of air (pure or containing variable contaminant vapors) can be introduced in this cell by the filling aperture and also can be eliminated by other aperture (Fig. 5).

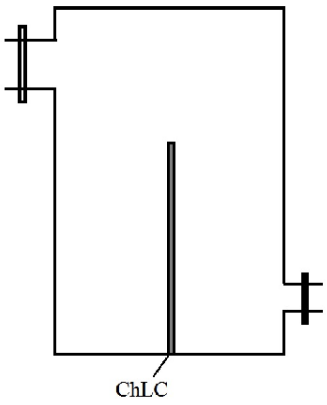

Fig. 5 – Cell containing Cholesteric liquid crystal embedded in polyurethane film.

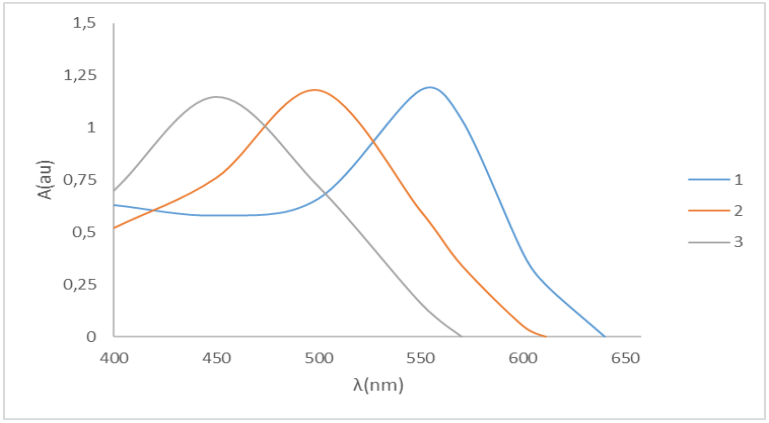

Fig. 6 – Electronic absorption spectra of Cholesteric liquid crystal in the presence of tetrahydrofuran vapors (1 – C=0; 2 – C=0.1%; 3 – C=0.2%).

The electronic absorption spectra of the cell were recorded at a Specord UV Vis spectrophotometer with data acquisition system. The absorption band of cholesteric liquid crystal was shifted to small wavelengths when the pollutant concentration increased (Fig. 6).

Our experimental data refer to tetrahydrofuran (THF) vapors introduced in increasing quantities in the air jet. The concentration of the THF vapors was under 0.2%. A gradual decreasing in the wavelength was observed when the THF vapor concentration was increased, as one can see in Fig. 7.

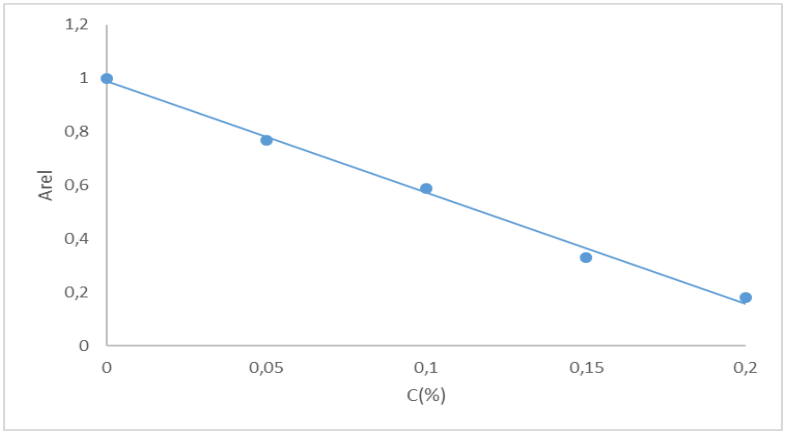

Fig. 7 – Dependence of the absorption band position in the wavelength scale on the THF vapor concentration.

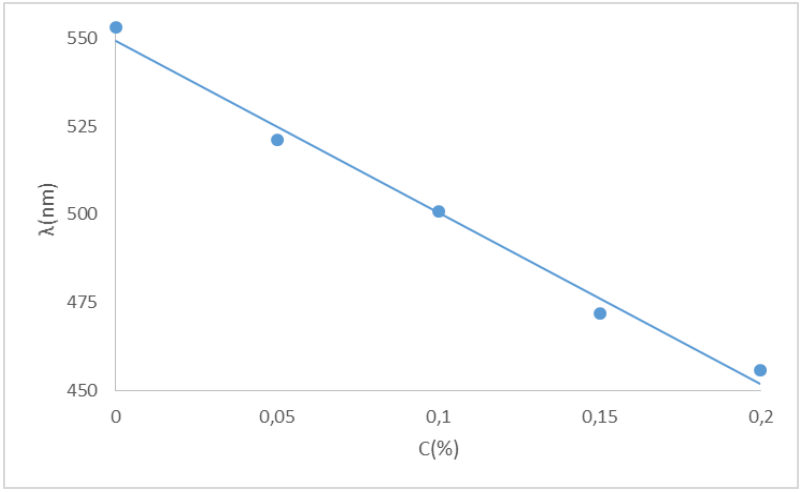

Fig. 8 – Dependence of the relative absorption measured at a fixed wavelength on the vapor concentration.

If one measure the absorbance at a fixed wavelength, for example at 553 nm corresponding to the cell spectrum in the absence of the contaminant vapor, the increase in the relative absorbance is monitored (Fig. 8). The relative absorbance is defined as the ratio between the absorbance measured in the contaminant vapors presence and the absorbance (measured at the same wavelength) in the absence of the contaminant vaporous.

As it results from Figs. 7 and 8, using a thin Cholesteric layer embedded in a polymer, very small amounts of contaminant vapors can be detected using the spectral information.

5. Applications of Cholesteric Liquid Crystals. Technical Devices

Due to their marked photo stability, reversibility and high sensitivity, cholesteric liquid crystals offer widespread applications as sensor materials, for detection of solvent polar molecules without pronounced reactivity.

As it was demonstrated (Mujahid *et al*., 2010), cholesteric materials are able to discriminate between different polar solvents. A nearly linear dependence between the absorbance A and the molar mass of the polar solvent at passing its vaporous through a cholesteric liquid crystals layer is established by Mujahid and his co- workers. The measurements were made with cholesteric liquid crystals encapsulated in a polystyrene matrix. The cholesteric liquid crystals in the imprinted polymer matrix provide selectivity for solvent vaporous detection. The weight and the chemical structure of the solvent influence the pitch of the cholesteric liquid crystals, and so, one can change the absorbed light spectral composition. Small amounts of contaminants are detected in the atmosphere with devices containing cholesteric liquid crystalline layers described by Shibaev and his co-workers (Shibaev *et al.*, 2015).

Cholesteric liquid crystals are thermochromic materials that change their color over a wide range of temperatures from as low as -30^{o}C to far above 100^{o}C. These limits are delimited by crystallization at low temperatures and by the stability of liquid crystal and also by the stability and lifetime of the device itself.

Thermochromic devices have considerable advantages over other thermometers in that they are cheap, flexible, virtually unbreakable and easy to read.

The ability to monitor and to map the temperature of a surface area recommends the thermochromic liquid crystals for engineering applications. For example, in electronics, cholesteric liquid crystals can be used to detect short circuits, open circuits, inoperative devices, or to map operational in integrated circuits. The defects of materials, causing an interruption in thermal conductivity can be also evidenced using cholesteric liquid crystals.

Thermography based on liquid crystals was used in evaluation of thermal transfer between fluids and solid surfaces (Ireland and Jones, 1985) and also in mapping local temperature variations in a flowing fluid (Wozniak and Wozniak, 1991; Stasiek and Kowalewski, 2002).

4. Conclusions

Firstly recognized mesophases**,** cholesterics form the basis of widespread liquid crystals devices and they continue to find new applications in high- technology.

The change in pitch under small variations of pressure, temperature, or in presence of contaminants recommends cholesteric liquid crystals as rapid and regular products for thermometers and very sensitive materials for detection of noxious vapor detection.

REFERENCES

Brown G.H., Doane W.J., Neff V.D., *A Review of Structure and Physical Properties of Liquid Crystals*, CRC Press, Cleveland Ohio, 1971.

Bunning T., Chen S., Harthorne N., Kajiyama T., Koide N., *Liquid Crystals for Advances Technologies*, Materials Research Society, Pitsburg, 1996.

Collings P., Hird M., *Introduction to Liquid Crystals – Chemistry and Physics*, Taylor and Francis, 1997.

De Gennes P.G., *The Physics of Liquid Crystals*, Claredon, Oxford, 1974.

Demus D., Lothar R., *Textures of Liquid Crystals*, Deutscher Verlag fur Grundstoffindustrie, Leipzig, 1978.

Demus D., Goodby J.W., Gray G.W., Spices H.W., Vill V. (Eds.), *Handbook of Liquid Crystals Fundamentals,* Wiley VCH, Weinheim, 1998.

Dumitrașcu I., Dorohoi D.O., *Optical Anisotropy*. Applications, Ed. Tehnopress, Iași, 2015.

Kleinert H., Maki K., *Lattice Textures in Cholesteric Liquid Crystals*, Fortschritte der Physics, **29**, 219-259 (1981).

Ireland P., Jones T., *Heat Transfer and Cooling in Gas Turbines*, AGARDCD – 390, Bergen, Norway, 1985.

Meier G., Seckmann E., Grabmaier J.G., *Applications of Liquid Crystals*, Springer, Verlag, Berlin, 1975.

Moțoc I., Muscutariu I., *Introducere în Fizica Cristalelor Lichide*, Edit. Facla, Timișoara, 1986.

Mujahid A., Stathopulos H., Lieberzeit P.A., Dickert F.L., *Solvent Vapour Detection with Cholesteric Liquid Crystals* - Optical and Mass – Sensitive Evaluation of Sensors Mechanism, Sensors, **10**, 4887-4897 (2010).

Muscutariu I., *Cristale Lichide și Aplicații*, Edit. Tehnică, București, 1981.

Pershan P.S., *Structure of Liquid Crystals Phases*, *Word Scientific*, Singapore, 1978.

Shibaev P.V., Wenzlick M., Murray J., Tantillo A., Howard – Jennings J., *Rebirth of Liquid Crystals for Sensoric Applications: Environmethal and Gas Sensors*, Advanced in Condensed Matter Physics, Vol. 2015, http://dx.doiorg/10.1155/2015/729186.

Stasiek J.A., Kowalewscki T.A., *Thermotropic Liquid Crystals Applied for Heat Transfer Research*, Opto-Electronics Review, **10**, *1*, 1-10 (2002).

Wozniak G., Wozniak K., *Simultaneous Measurements of Temperature and Velocity Fields in Thermo-Conductive Liquid Flows – Development of New Measuring Technique*, Monography Research; Material and Fluid Science, Adv. Space Res., **11**, 33-38 (1991).

CRISTALE LICHIDE COLESTERICE ȘI APLICAȚIILE LOR ÎN MĂSURAREA TEMPERATURILOR ȘI ÎN DETECȚIA CONTAMINĂRII CU VAPORI

(Rezumat)

Cristalele lichide colesterice formează filme subțiri cu proprietăți optice speciale. Sensibilitatea lor la schimbări de temperatură oferă posibilitatea măsurării unor variații mici de temperatură sau a evidențierii diferitelor unde mecanice sau electromagnetice datorită efectelor lor calorice.

Cantități mici de vapori contaminanți din atmosferă pot fi detectate cu dispozitive conținând cristale lichide colesterice datorită sensibilității ridicate a pasului colestericului la impurități. Un studiu experimental pentru evidențierea vaporilor de tetrahidrofuran a fost realizat cu un cristal lichid colesteric încapsulat în matrice poliuretanică.

BULETINUL INSTITUTULUI POLITEHNIC DIN IAŞI
Publicat de
Universitatea Tehnică „Gheorghe Asachi” din Iaşi
Volumul 63 (67), Numărul 1, 2017
Secţia
MATEMATICĂ. MECANICĂ TEORETICĂ. FIZICĂ

EXTERNAL STIMULATION IN NEURAL MATRIX RECOVERY

BY

CONSTANTIN COSTESCU*

“Vasile Alecsandri” University of Bacău,
Department of Mathematics

Received: February 7, 2017
Accepted for publication: March 30, 2017

Abstract. External stimulation of the skin generates different levels of activity in neural network, levels that can lead to neural regeneration matrix. These levels are coordinated by algorithms that generate epidermis stimulation. By observing the activity of neural network through 2D and 3D topographic analysis and time-frequency analysis, we can decide which functions of the algorithm must be maintained, updated or removed in order to have a maximum neural stimulation and reply. This analysis is intended to improve the initial set of data constituting the initial matrix in the process of neural stimulation and the forming of initial matrix for various neural disorders. The accuracy of these matrixes will decrease the response time of the patient with the applied stimulation algorithms and will improve the quality of response and motor cortex.

Keywords: algorithms; epidermis; sensors.

1. Introduction

Cerebrovascular accident (CVA) occurs when the blood flow to a part of the brain is stopped. CVA is categorized in ischemic or hemorrhagic: ischemic CVA occurs when the blockage stops the blood flow and hemorrhagic when a blood vessel suffers a rupture. Both ischemic and hemorrhagic CVA will reduce the blood flow and oxygen level in the portion of brain where CVA is located.

*Corresponding author; *e-mail*: c.costescu@gmail.com

Blocking the flow of blood to any part of the brain for just a couple of minutes will lead to the death of neural endemic cell (not only) and thus, the affected areas will reduce their functions and activities (Duvinage *et al*., 2013; Kandel *et al*., 2000).

This raises a question. Is reducing the activity not a reversible process somehow? Perhaps these functions can be active again once the creation and initialization of initial operating conditions take place. Can the functional memories and the functions once thought lost be reversed, not only by setting initial conditions, but also by rebuilding the entire process of learning?

When the motor cortex is damaged, neuromotor functions are diminished and so the patient will be unable not only to coordinate daily activities but also to determine recovery activities (Badcock *et al*., 2015; Graimann *et al*., 2010).

The actions to be taken in case of a CVA, regardless of its type, hemorrhagic or ischemic, require rapid intervention and not just medication. Non-action after CVA can generate permanent damage to brain function, permanent disabilities, most often without being able to be remedied within the life span of a patient suffering what CVA.

In support of these actions, the research of methods that can be used to stimulate the patient, correlated with the research of neural activity in response following stimulation, may show new methods of treatment and rehabilitation of the patients who suffered CVA.

Mathematical directed and coordinated stimulation on the patient's epidermal level after an initial matrix generates a response in the motor cortex areas F3, FC5. Thus, we highlight the function of stimulus defined on an initial matrix with values in the motor cortex.

2. Hardware Equipment

To demonstrate the existence of this function, we will use a device that generates mechanical impulses according to a reference matrix (initial matrix). The second part consists from mathematical modeling of signals emitted by the brain and captured with an EmotivEpoc + Row device, 14 channels.

The components are listed in the Table 1.

Table 1
Equipment's

Monitoring	Stimulation	Capturing
Lenovo T520		EpocEmotiv+ Row
Beagle Bone Black	StD	
4DCAPE-70T		

The operating system and the software packages are mentioned in the Table 2:

Table 2
Operating Systems

SO	Capturing	Modelation
Linux	Open Vibe	Open Vibe
Windows	Emotiv	Mat Lab
		Open EEG

External Stimulation Device (ESD) is the device that will convert the starting matrix into stimuli that will be applied on the patient. It consists of a Beagle Bone Black board running Linux, Debian distribution to which it is connected an electronic system StD (Fig. 1).

Its role is to read the initial matrixes and the replication of matrix values in impulses sent to the epidermis, through its connection with sensors L and R.

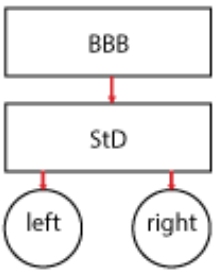

Fig. 1 – ESD - Main Board BBB, StD (hardware).

ESD can monitor the status of the patient by collecting data such as: temperature, luminous flux, movement of patient, etc. For monitoring, it is used Python, with the MathPlotLib library. For stimulus transmission, two vibrating elements, left - right are used.

When EDS is used in practice, it communicates directly with the patient and its role is to observe the most sensitive changes.

EmotivEpoc + is a device used for capturing the electrical activity of the brain, using 14 channels and two references. It is used to measure visual response and can be used to highlight the event related potential (ERP).

Epoc headset is composed of 14 sensors, two references, a wireless transmitter and sensors AF3, F7, F3, FC5, T7, P7, O1, O2, P8, T8, FC6, F4, F8, AF4. M1 and M2 act as ground reference point in order to be able to measure the output (Fig. 2).

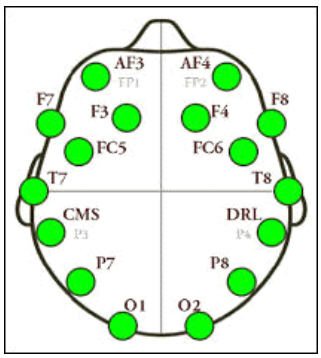

Fig. 2 – Electrodes.

Epoc uses a notch filter (50Hz-60Hz) and a low-pass hardware filter and the signal is sent with a resolution of 128 bits (Fig. 3).

Fig. 3 – EmotivEpoc+ Row device.

3. Theory

3.1. Calibration

The initial phase is to ensure a maximum relevant to the hardware device Epoc + , that will be used to reveal the samplings that will be analyzed and modeled mathematically.

Before starting to capture neural waves, the Epoc device must be calibrated because it does not have enough sensors on the middle area of the motor cortex and so the F3 and FC5 sensors must be repositioned, closer to the median on the Epoc device.

Once the F3 and FC5 sensors are positioned so that the reference of the signal function is positive and the Epoc device reports a positive level connection (green flag), we start to capture the first samples.

Once we have the first samples, we must ensure that these represent real, not fake, data even if the notifications reported by Epoc are green on each

of the sensors (this indicates that the sensors work in parameters and the captured signals can be modeled, representing the real data).

3.2. Capturing Neural Signals

In this stage, we intend to capture neural activity from all areas available allowed by Epoc + device, particularly in the AF3, F7, F3 and FC5 areas, that represents the maximum area of interest.

We note with N1 and N2 the samplings we obtain by capturing neural activity and with A1 and A2 the algorithms that will generate the external stimulation of the skin through the StD device. The ΔLAn is the notation for the time interval corresponding to the external stimulation for the left part – left hand stimulation and ΔRAn the time interval for the right part – right hand stimulation.

These data may be represented in the following table as we can see:

Table 3
StD Initial Data Set

Δ(L|R)A	L, [sec]	R, [sec]
	0.5	0.0
	1.0	1.0
	1.2	0
	0.0	1.0
	...	

In this stage, we seek to capture neural responses as function on the external stimuli generated by ESD and correlate them with the responses obtained from mathematical modeling performed on the obtained N1, N2 samplings.

This correlation will help us to create a stimulus - response (SR) correspondence, which associates a mathematically modeled response to the time period generated by the StD.

Thus, we can say that an Nkx response corresponds to an Akx interval and so, this response is due to external action generated by StD, where k = 1,2, x = 1,j, j <= N, N is the counter of values from Table 3. Table 3 has four values, so in this case N = 4. In practice, values of N are 30 – 50 in order to have sufficient external stimuli.

Next phase is to upload the algorithm in ESD, start the ESD and capture the brain electric signals.

ESD will generate left-right external stimulations following the next flow that has the distribution: ID, BL, TL, BR, TR.

ID = Stimulation ID,
BL = 1; 0-0 stop; 1 send stimulus on the left,
BR = 1; 0-0 stop; 1 send right stimulus,
TL = float (x, y) - the number of seconds in which the left side stimulus is activated,
TR = float (x, y) - the number of seconds in which the right side stimulus is activated.

And so, a string of this form:
0, 1.2, 1, 1.5 means only right side stimulation for a period of 1.5 sec.

While a string of the form:
1, 0.5, 1, 0.7 means left side stimulation for 0.5 sec and right side stimulation for 0.7 sec.

For obtaining the N1 and N2 samplings, Epoc + is initialized and OpenVibe is started. OpenVibe will capture neural flows and it will save them in the OpenVibe format. For this, we use a simple script that reads data from Epoc + driver and converts it into an open format with Vibe.

In this way, samplings (data) will be loaded into the modeling phase and the results will be associated with the Ax intervals corresponding to each stimulus applied to the skin. The stimulus will generate neural feedback and this will prove that to the intervals: delta la and delta ra correspond specific neural feedbacks. These feedbacks will prove changes in the neural matrix, generated by external stimulation.

3.3. Mathematical Modeling

This step involves the existence of N1, N2 samplings obtained from external stimulation with the evaluation of the response in the motor cortex.

To analyze these samplings, we will use the OpenVibe application in which a scenario S will be created which when running on samplings N1, N2 will show (Fig. 4):

Fourier distribution on the areas F3, FC5
2D Topographic Map - VC1
Time Frequency Map - VC2
Mathematical modeling of samplings lies in:
The reading of the samplings saved in GDF
Filtering the signals depending on the frequency of study (0, 12 Hz, 12-17 Hz)
Spectral analysis (FFT)
Data display
2D Topographic Map
TFM - Time Frequency Map

The scenario thus defined will run on the files obtained (Sampling files) and we will see each result Pk, k = 1, n, n <= N (N = number of datasets from Table 3) that correlates the time of OpenVibe with the StD time.

To be reminded that this correlation is possible because the start time was synchronized with StD and data logging using Epoc +.

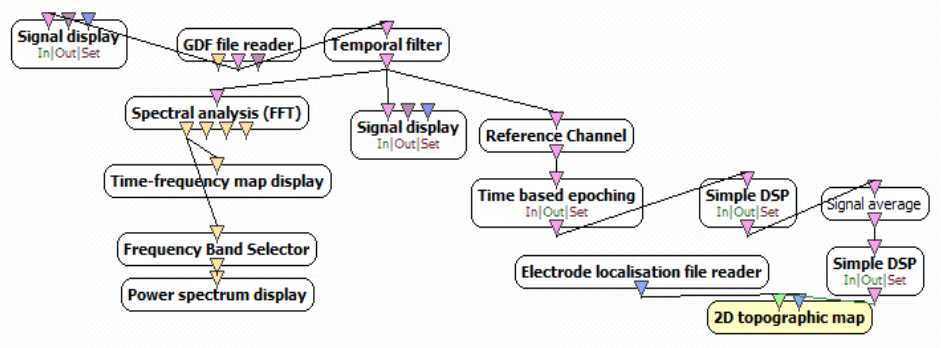

Fig. 4 – Scenario.

With Epoc + device configured, calibrated, initialized, ready for recording, the StD is started and Delta StD is withheld from OpenVibe. Now is possible the correlation between the events X noticed by modeling and the StD time, when the external stimulation is held.

By running scenario S on the samplings Nk (k = 1.2 in this case) we will be able to observe changes which took place in the motor cortex. These observations are made by detecting changes in VCSi, VCTi, VTTi, where:

VCS_i – Signals at the time T_i, from sampling N_k (Fig. 5)

VCT_i – 2D Topography at the time T_i, of sampling N_k (Fig. 6)

VTT_i – Time Frequency Map at the time T_i, from sampling N_k (Fig. 7)

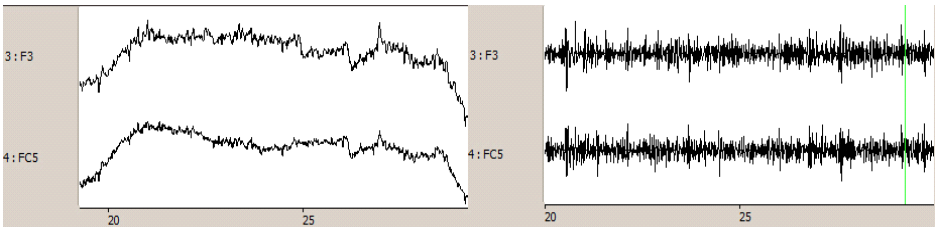

Fig. 5 – Signals – VCS_i, i = 1.

By comparing the time periods when changes occur in the cortex with the time periods from Table 3, we find that there is a correlation between these

events, so we can infer that the observed changes in the motor cortex are due to the external stimuli of StD.

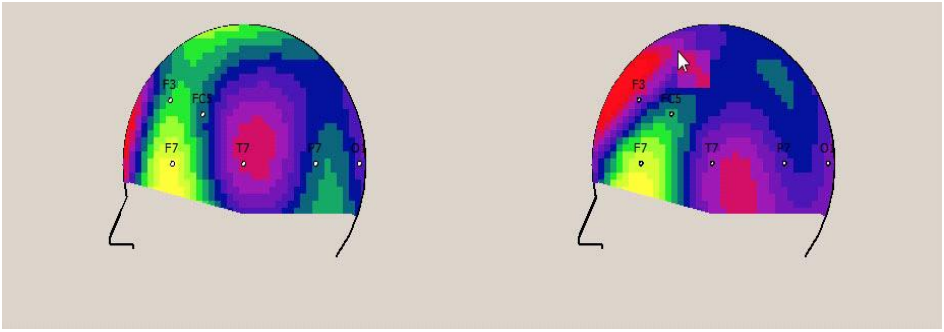

Fig. 6 – 2D Topography – VCT_i, i = 1.

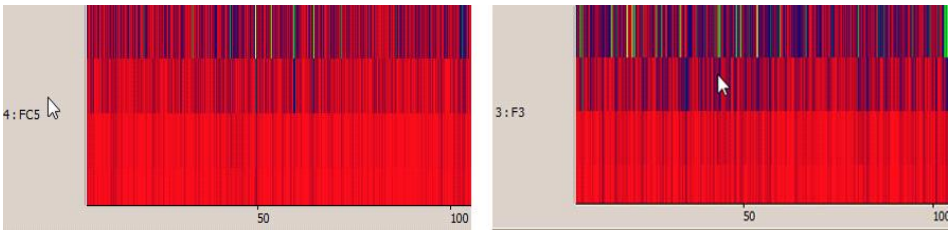

Fig. 7 – TFM 2CH – VTT_i, i = 1.

The next stage is to analyze whether the changes that we observe through the shaping of the motor cortex activity may be correlated with stimulation times defined in ESD for the A_{left} and A_{right} values.

If until now we have shown that the external stimulation produces changes in the motor cortex, we intend to show that these changes can be coordinated according to the algorithm tried in ESD.

Thus, a series of the form

$$\prod_{k=1}^{n} AL_k \,|AR_k \tag{1}$$

where AL_k is the value for the left side and AR_k is the value for the right side, will determine the distinct electrical activity, depending on the AL_k and AR_k value changing.

This change in the motor cortex activity, dependent on the values of external left and right stimulation, makes us propose to find the values for which the CM activity is maximum.

These values can complete Table 3 or can even replace the initial data of the table, becoming thus the standard protocol for starting the restoring CM program.

It is recommended like these changes be backed up by observations on the state of patients on which stimulus and PET analysis algorithms will be applied as a more objective picture of the state and patients evolution.

Depending on the input algorithms and the observations on patients, arrays of initial data can be defined. These can be loaded in StD depending on the initial state of the patient and according to initial medical evaluation.

4. Conclusions

External stimulation in the epidermis involves motor cortex activity responses, responses that are driven mostly by changes during left right stimulation.

The initial start matrix has to be updated in order to obtain the maximum result from the CM activity. In the update process, the observation and the evolution of the patient have an important role. Also, the changes to the CM obtained by PET scan are important.

The sum of these observations, their conversion into start matrixes and their segmentation depending on the types of neural disorders constitute the main engine in medical rehabilitation of patients.

The external stimuli used in this experiment were rudimentary, but nonetheless the results confirm the theory of generating an activity to the CM through mathematically directed and coordinated external stimulation. The use of external stimulation equipment (equipment that can generate quick response feelings) leads to the improvement of algorithms and patient response and thus to an improvement of motor activity in the process of recovery and medical rehabilitation.

The notions presented are the basis of building a medical device that can provide a viable solution in the process of recovery and medical rehabilitation, a process that is treated most often with indifference in the wake of CVA or other neural dysfunction.

Along with running multiple experiments to obtain initial data matrices (for implementation in StD) changes can be observed at the state of patients suffering from Alzheimer, etc.

Following tests and establishing data matrices, the StD system can run by itself on the patient, the data gathered about patient's progress being sent to a server that will change algorithms depending on patient progress.

In this way, patients who have suffered a CVA or neural dysfunction may have the chance of recovery and rehabilitation considering that this process does not require high costs and the fact that this process of recovery and rehabilitation is continuous 24/7/365.

REFERENCES

Badcock N.A., Preece K.A., de Wit B., Glenn K., Fieder N.,Thie J., McArthur G., *Validation of the Emotiv EPOC EEG System for Research Quality Auditory Event-Related Potentials in Children*, PeerJ, Vol. **3** (2015), https://www.ncbi.nlm.nih.gov/pmc/articles/PMC4411518/.

Duvinage M., Castermans T., Petieau M., Hoellinger T., Cheron G., Dutoit T., *Performance of the EmotivEpoc headset for P300-Based Applications*, BioMedical Engineering OnLine 2013, biomedical-engineering-online.biomedcentral.com/articles/10.1186/1475-925X-12-56.

Graimann B., Allison B.Z., Pfurtscheller G., *Brain-Computer Interfaces Revolutionizing Human Computer Interaction*, Spriger, New York (2010).

Kandel E.R., Schwartz J.H., Jessell T.M., *Principles of Neural Science*, New York, McGraw-Hill, Health Professions Division (2000).

STIMULAREA EXTERNĂ ÎN RECUPERAREA MATRICII NEURONALE

(Rezumat)

Stimularea externă la nivelul epidermei generează diferite nivele de activitate în rețeaua neuronală, nivele ce pot duce la regenerarea matricii neuronale. Aceste nivele sunt coordonate de algoritmii care generează stimularea epidermului. Astfel, prin observarea activității neuronale, și anume prin analiza topografică 2D, 3D și timp-frecvență putem decide care dintre funcțiile algoritmului trebuie menținută, actualizată sau înlăturată, pentru a avea un maxim de stimulare neuronală și răspuns. Această analiză are rolul de a îmbunătăți setul inițial de date ce constituie matricea inițială în procesul de stimulare neuronală și de formare a matricii inițiale pentru diverse tipuri de afecțiuni neuronale. Acuratețea acestor matrici va duce la micșorarea timpului de răspuns al pacientului pe care se aplică algoritmii de stimulare pentru îmbunătățirea răspunsului și calității cortexului motor.

BULETINUL INSTITUTULUI POLITEHNIC DIN IAŞI
Publicat de
Universitatea Tehnică „Gheorghe Asachi” din Iaşi
Volumul 63 (67), Numărul 1, 2017
Secţia
MATEMATICĂ. MECANICĂ TEORETICĂ. FIZICĂ

INTEGRABILITY IN INTERVAL-VALUED (SET) MULTIFUNCTIONS SETTING

BY

ALINA IOSIF[1,*] and ALINA GAVRILUŢ[2]

[1]Petroleum-Gas University of Ploieşti,
Department of Computer Science, Information Technology, Mathematics and Physics
[2]“Alexandru Ioan Cuza” University of Iași,
Faculty of Mathematics

Received: February 18, 2017
Accepted for publication: March 30, 2017

Abstract. We recently proposed a new integral of an interval-valued multifunction relative to an interval-valued set multifunction. In this paper we continue the study of this type of integral, establishing various specific properties. Some properties regarding Gould type integrability on atoms are also discussed.

Keywords: gould integral; interval valued (set) multifunction; submeasure; multisubmeasure; non-additive set function; monotone measure.

1. Introduction

The theory of fuzzy sets was introduced by Zadeh (1968). Since then many new theories came out, such as the interval-valued fuzzy sets theory, the generalized theory of uncertainty etc. During the last decade, it has been suggested to use intervals in order to represent uncertainty in the area of decision theory and information theory, for example, calculation of economic uncertainty, theory of interval probability as a unifying concept for uncertainty.

*Corresponding author; *e-mail*: emilia.iosif@upg-ploiesti.ro

Thus, a special attention was recently paid to the study of interval-valued (set) multifunctions, since they are related to the representation of uncertainty, a necessity coming from economic uncertainty, fuzzy random variables, interval-probability, martingales of multivalued functions, interval-valued capacities, interval-valued intuitionistic fuzzy sets (Bykzkan and Duan, 2010; Jang, 2004; Jang, 2006; Jang, 2007; Jang, 2011; Jang, 2012; Tan and Chen, 2013; Qin *et al*., 2016; Bustince *et al*., 2013 - in multicriteria decision making problems, Li and Sheng, 1998; Li *et al*., 2014; Weichselberger, 2000 and many others).

Entropy, the well-known concept in physics, information theory and fuzzy set theory, describes the degree of uncertainties and fuzziness of the fuzzy sets. Precisely, entropy and similarity of intuitionistic fuzzy sets are very important in theory and applications in which the intuitionistic fuzzy sets are used to describe the imprecisions and uncertainties.

On the other hand, set-valued functions theory has become an important tool in several practical areas, especially in economic analysis, where it treats problems of individual demand, mean demand, competitive equilibrium, coalition production economies etc. For instance, applications of integration of set-valued functions in economy analysis have roots in Aumann's (1965) research based on the classical Lebesgue integral.

Different types of integrals have been introduced and studied in order to generalize the Riemann integral. In this framework, a way of defining the integral is to use finite or infinite Riemann type sums as in, for instance (Aviles *et al*., 2010; Birkhoff, 1935; Boccuto and Sambucini, 2004; Boccuto and Sambucini, 2012; Boccuto *et al*., 2014; Cascales and Rodriguez, 2004; Dinghas, 1956; Fremlin, 1995; Gould, 1965; Sipos, 1979; Spaltenstein, 1995). An influential work in this direction was Gould's study, 1965, where the concept of an integral using finite sums for real functions with respect to finitely additive vector measures, is introduced.

The Gould integral was generalized and studied in (Gavriluț and Petcu, 2007a; Gavriluț and Petcu, 2007b; Gavriluț *et al.*, 2014) (relative to submeasures), Precupanu and Croitoru, 2002; Precupanu and Croitoru, 2003; Precupanu and Satco, 2008) (relative to multimeasures), (Gavriluț, 2008; Gavriluț, 2010; Sofian-Boca, 2011) (relative to multisubmeasures), (Precupanu *et al*., 2010) (relative to monotone set-valued set functions).

A special type of an interval-valued set multifunction was introduced by Sofian-Boca (2011), with respect to the order relation of Guo and Zhang (2004), in order to study a Gould type integral of a real function with respect to it. This type of set multifunction was also investigated by Gavriluț (2014). In (Jang, 2004; Jang, 2006; Jang, 2007; Jang, 2011; Jang, 2012; Tan and Chen, 2013; Qin *et al*., 2016; Bustince *et al*., 2013) are studied the interval-valued (intuitionistic fuzzy) Choquet integrals and also pointed out their applications in multicriteria decision making problems. Also, in (Hamid and Elmuiz, 2016), the Henstock-Stieltjes integrals of interval-valued functions and fuzzy-number-valued functions are introduced.

In this paper, we continue the study of our new integral (Pap *et al*., submitted for publication) of an interval-valued multifunction relative to an interval-valued set multifunction, pointing out various important properties of it. Indeed, due to this integration type specific, one would expect to obtain special properties.

The paper is organized as follows: Section 1 is for introduction. After Section 2 (of basic concepts, various examples and results), in Section 3 we obtain some remarkable properties of the Gould integral of interval-valued multifunctions relative to a interval-valued set multifunctions. Also, we prove some results regarding Gould type integrability on atoms.

2. Preliminaries

If $n \in \mathrm{N}^*$, by $i = \overline{1,n}$ we mean $i \in \{1,...,n\}$. All over this paper, let be $\mathrm{R}_+ = [0,\infty)$, T a nonempty abstract set, $\mathrm{P}(T)$ the family of all subsets of T and A an arbitrary algebra of subsets of T.

Definition 1. *A finite partition of T is a finite family of nonempty sets $P = \{A_i\}_{i=\overline{1,n}} \subset \mathrm{A}$ such that $A_i \cap A_j = \varnothing, i \neq j$ and $\bigcup_{i=1}^{n} A_i = T$.*

We denote by $\mathrm{P}(T)$ the class of all partitions of T and by P_{A}, the class of all partitions of A, if $\mathrm{A} \in \mathrm{A}$ is fixed.

Definition 2. (*i*) *If P, $P' \in \mathrm{P}$, P' is said to be finer than P (denoted by $P \leq P'$ or $P' \geq P$) if every set of P' is included in some set of P.*

(ii) *The common refinement of two finite partitions $P = \{\mathrm{A}_i\}_{i=\overline{1,n}}$, $P' = \{B_j\}_{j=\overline{1,m}} \in \mathrm{P}$ is the partition $P \wedge P' = \{A_i \cap B_j\}_{\substack{i=\overline{1,n} \\ j=\overline{1,m}}}$.*

Let be an arbitrary set function $m : \mathrm{A} \to \mathrm{R}_+$, with $\mathrm{m}(\varnothing) = 0$.

Definition 3. (Pap, 1995) I. *m is said to be:*

(i) *monotone (*or, *fuzzy)* if $m(A) \leq m(B)$, for every $A, B \in \mathrm{A}$, with $A \subseteq B$;

(ii) *subadditive* if $m(A \cup B) \leq m(A) + m(B)$, for every (disjoint) $A, B \in \mathrm{A}$;

(iii) a *submeasure* (in the sense of Drewnowski (1972)) if it is monotone and subadditive;

(iv) *null-additive* if $m(A \cup B) = m(A)$, for every $A, B \in \mathrm{A}$, with $m(B) = 0$;

(v) σ *-subadditive* if $m(A) \leq \sum_{n=0}^{\infty} m(A_n)$, for every (pairwise disjoint) $(A_n)_{n\in \mathrm{N}} \subset \mathrm{A}$, with $A = \bigcup_{n=0}^{\infty} A_n \in \mathrm{A}$;

(vi) *finitely additive* if $m(A \cup B) = m(A) + m(B)$, for every disjoint $A, B \in \mathrm{A}$;

(vii) σ *-additive* if $m(\bigcup_{n=0}^{\infty} A_n) = \sum_{n=0}^{\infty} m(A_n)$, for every pairwise disjoint $(A_n)_{n\in \mathrm{N}} \subset \mathrm{A}$;

II. A set $A \in \mathrm{A}$ is *an atom with respect to m* if $m(A) > 0$ and for every $B \in \mathrm{A}$, with $B \subset A$, we have either $m(B) = 0$ or $m(A \setminus B) = 0$.

III. m is said to be *finitely purely atomic* if $T = \bigcup_{i=1}^{p} A_i$, where $A_i \in \mathrm{A}$, $i = \overline{1, p}$ are pairwise disjoint atoms of m.

Definition 4. (i) *The variation* $\overline{m}$ *of* m *is the set function* $\overline{m} : \mathrm{P}(T) \to 0, +\infty]$ *defined by* $\overline{m}(E) = \sup\{\sum_{i=1}^{n} m(A_i)\}$, *for every* $E \in \mathrm{P}(T)$, *where the supremum is extended over all finite families of pairwise disjoint sets* $\{A_i\}_{i=1}^{n} \subset \mathrm{A}$, *with* $A_i \subseteq E$, *for every* $i = \overline{1, n}$.

(ii) m is said to be *of finite variation on* A if $\overline{m}(T) < \infty$.

Remark 5. I. If $E \in \mathrm{A}$, then in the definition of $\overline{m}$ one may consider the supremum over all finite partitions $\{A_i\}_{i=1}^{n} \in \mathrm{P}_E$.

II. $\overline{m}$ is monotone on $\mathrm{P}(T)$.

III. If m is finitely additive, then $\overline{m}(A) = m(A)$, for every $A \in \mathrm{A}$.

IV. If m is subadditive ($\sigma -$ subadditive, respectively) of finite variation, then $\overline{m}$ is finitely additive (σ -additive, respectively) on A .

We denote by $\mathrm{P}_0(\mathrm{R}_+)$ the family of all nonempty subsets of R_+ and by $\mathrm{P}_{kc}(\mathrm{R}_+)$ the family of nonempty, compact convex subsets of R_+ .

Definition 6. (Guo and Zhang, 2004) *(the "standard" partial order relation* $''\preccurlyeq''$ *on* $\mathrm{P}_0(\mathrm{R}_+)$, *which extends the usual order on* $\mathrm{P}_{kc}(\mathrm{R}_+)$*): If* $A, B \in \mathrm{P}_0(\mathrm{R}_+)$, *then* $A \preccurlyeq B$ *if the following two conditions hold:*

(i) for every $x \in A$, there exists $y_x \in B$ so that $x \le y_x$;

(ii) for every $y \in B$, there exists $x_y \in A$ so that $x_y \le y$.

In general, there is no implication between the order relation $''\preccurlyeq''$ and the inclusion one. However, on the family $\{[0,a]; 0 \le a < \infty\}$ they coincide. By convention, $\{0\} = [0,0]$.

If $[a,b],[c,d] \in \mathrm{P}_{kc}(\mathrm{R}_+)$, the following operations are considered (see (Jang, 2007) for details):

I. $[a,b]+[c,d] = [a+b, c+d]$;

II. $\alpha \cdot [a,b] = [\alpha a, \alpha b], \alpha \ge 0$;

III. $[a,b] \cdot [c,d] = [a \cdot c, b \cdot d]$;

IV. $[a,b] \wedge [c,d] = [\min\{a,c\}, \min\{b,d\}]$;

V. $[a,b] \vee [c,d] = [\max\{a,c\}, \max\{b,d\}]$;

VI. $[a,b] \subseteq [c,d]$ if and only if $c \le a \le b \le d$;

VII. $[a,b] \preccurlyeq [c,d]$ if and only if $a \le c$ and $b \le d$.

On $\mathrm{P}_0(\mathrm{R})$ we consider the Hausdorff-Pompeiu pseudo-metric h (Hu and Papageorgiou, 1997) defined for every $A, B \in \mathrm{P}_0(\mathrm{R})$ by

$$h(A,B) = \max\{\sup_{x\in A}\inf_{y\in B} |x-y|, \sup_{y\in B}\inf_{x\in A} |x-y|\}.$$

On $\mathrm{P}_{kc}(\mathrm{R}), h$ has the particular form:

$$h([a,b],[c,d]) = \max\{|a-c|, |b-d|\}, \forall a,b,c,d \in \mathrm{R}, a \le b, c \le d.$$

According to (Hu and Papageorgiou, 1997), $(\mathrm{P}_{kc}(\mathrm{R}), h)$ is a complete metric space.

For every $M \in \mathrm{P}_{kc}(\mathrm{R}), M = [a,b]$, we denote

$|M| = h(M,\{0\}) (= \max\{|a|, |b|\})$.

If, particularly, $0 < a < c$, then $h([0,a],[0,c]) = c - a$.

If $M \in \mathrm{P}_{kc}(\mathrm{R}_+), M = [a,b]$, then $|M| = b$.

We now recall from (Pap *et al.*, submitted for publication) several notions (in the set-valued case) defined with respect to $''\preccurlyeq''$ on $\mathrm{P}_0(\mathrm{R}_+)$:

Definition 7. *Let* $\mu : \mathrm{A} \to \mathrm{P}_0(\mathrm{R}_+)$ *be a set multifunction, with* $\mu(\varnothing) = \{0\}$.

I. μ is said to be:

(i) *an additive multimeasure* if $\mu(A \cup B) = \mu(A) + \mu(B)$, for every disjoint $A, B \in \mathrm{A}$;

(ii) *q-monotone* if $\mu(A) \preccurlyeq \mu(B)$, for every $A, B \in \mathrm{A}$, with $A \subseteq B$;

(iii) *q-subadditive* if $\mu(A \cup B) \preccurlyeq \mu(A) + \mu(B)$, for every disjoint $A, B \in \mathrm{A}$;

(iv) *aq-multisubmeasure* if it is q-monotone and q-subadditive;

(v) *null-additive* if $\mu(A \cup B) = \mu(A)$, for every $A, B \in \mathrm{A}$, with $\mu(B) = \{0\}$;

II. $A \in \mathrm{A}$ is *a q-atom of* μ if $\{0\} \preccurlyeq \mu(A), \{0\} \neq \mu(A)$ and for every $B \in \mathrm{A}$, with $B \subseteq A$, we have either $\mu(B) = \{0\}$ or $\mu(A \setminus B) = \{0\}$.

III. μ is said to be *finitely purely q-atomic* if $T = \bigcup_{i=1}^{p} A_i$, where $A_i \in \mathrm{A}$, $i = \overline{1, p}$ are pairwise disjoint q-atoms of μ.

Remark 8. Acccording to (Gavriluț, 2014), $\mu : \mathrm{A} \to \mathrm{P}_{kc}(\mathrm{R}_+)$ if and only if there exist two set functions $m_1, m_2 : \mathrm{A} \to \mathrm{R}_+$ so that for every $A \in \mathrm{A}$, $m_1(A) \leq m_2(A)$ (here " $\leq$ " is the usual order on R) and $\mu(A) = [m_1(A), m_2(A)]$. Moreover, in this case, μ is q-monotone, q-subadditive, q-multisubmeasure, null-additive (in the sense of the previous definition) if and only if both m_1, m_2 are monotone, subadditive, submeasures, null-additive, respectively, in the sense of Definition 3.

One can easily generate a q-multisubmeasure (in the sense of (Sofian-Boca, 2011) - see also (Gavriluț, 2014):

Example 9. If $\nu : \mathrm{A} \to \mathrm{R}_+$ is finitely additive, then $m_1, m_2 : \mathrm{A} \to \mathrm{R}_+$, defined by $m_1(A) = \sqrt{\nu(A)}$ and $m_2(A) = \dfrac{\nu(A)}{1 + \nu(A)}$, for every $A \in \mathrm{A}$ are submeasures (Gavriluț, 2012). In consequence, $\mu : \mathrm{A} \to \mathrm{P}_{kc}(\mathrm{R}_+)$, defined by $\mu(A) = [m_1(A), m_2(A)]$, $\forall A \in \mathrm{A}$ where m_1 and m_2 are as before, is a q-multisubmeasure.

Remark 10. I. A set $A \in \mathrm{A}$ is a q-atom of μ if and only if it is an atom of both m_1 and m_2 (in the sense of Definition 3-II).

II. Suppose μ is null-additive and has q-atoms. If A is a q-atom of μ, then every $B \in \mathrm{A}$, with $B \subseteq A$ and $\{0\} \prec \mu(A)$, is also a q-atom of μ and $\mu(A \setminus B) = \{0\}$, so $\mu(A) = \mu(B)$ also holds.

III. $\overline{\mu} = \overline{m_2}$ (on A).

IV. If μ is a q-multisubmeasure and if $A \in \mathrm{A}$ is a q-atom of μ, then $\overline{\mu}(A) = |\mu(A)| \, (= m_2(A) = \overline{m_2}(A))$.

3. Gould Integrability

In this section, we point out some remarkable properties of the Gould integral introduced in (Pap *et al*., submitted for publication) for interval-valued multifunctions with respect to an interval-valued set multifunction. Also, we provide different properties regarding Gould type integrability on atoms.

First we recall from (Gould, 1965), the definitions of totally-measurability and Gould integrabiliy of a real function with respect to a set function.

Let $m:\mathrm{A}\to\mathrm{R}_+$ be a non-negative set function, with $m(\varnothing)=0$. Let also $f:T\to\mathrm{R}$ be a real function.

Definition 11. (Gould, 1965) I. *f is said to be $\overline{m}$-totally measurable* (*on* (T,A,m)) *if for every* $\varepsilon>0$, *there exists* $P_\varepsilon=\{A_i\}_{i=\overline{0,n}}\subset\mathrm{A}, P_\varepsilon\in\mathrm{P}(T)$ *such that:*

(i) $\overline{m}(A_0)<\varepsilon$ and

(ii) $osc(f,A_i)=\sup\limits_{t,s\in A_i}|f(t)-f(s)|<\varepsilon$, for every $i=\overline{1,n}$.

II. f is said to be $\overline{m}$-*totally measurable on* $B\in\mathrm{A}$ if the restriction $f|_B$ of f to B is $\overline{m}$-totally measurable on (B,A_B,m_B), where $m_B=m|_{\mathrm{A}_B}$ and $\mathrm{A}_B=\{A\cap B;A\in\mathrm{A}\}$.

We consider $\sigma_{f,m}(P)$ (or $\sigma(P)$, for short) $=\sum\limits_{i=1}^{n}f(t_i)m(A_i)$, for every $P=\{A_i\}_{i=\overline{1,n}}\in\mathrm{P}(T)$ and every $t_i\in A_i, i=\overline{1,n}$.

Definition 12. (Gould, 1965) I. *f is said to be Gould m-integrable on T if the net $(\sigma(P))_{P\in(\mathrm{P}(T),\leq)}$ is convergent in* R. *In this case, its limit is called the Gould integral of f on T with respect to m, denoted by* $\int_T f dm$.

II. *f is said to be Gould m-integrable on $B\in\mathrm{A}$ if the restriction $f|_B$ is Gould m-integrable on* $(B,\mathrm{A}_\mathrm{B},\mu_B)$.

Remark 13. I. If it exists, the integral of f is unique.

II. f is Gould m-integrable on T if and only if there exists $\alpha\in\mathrm{R}$ such that for every $\varepsilon>0$, there exists $P_\varepsilon\in\mathrm{P}(T)$, so that for every other $P=\{A_i\}_{i=\overline{1,n}}\in\mathrm{P}(T)$, with $P\geq P_\varepsilon$ and every $t_i\in A_i$, $i=\overline{1,n}$, we have $|\sigma(P)-\alpha|<\varepsilon$.

We now recall from (Pap *et al*., submitted for publication) the notions of total-measurability and Gould integrability for an interval-valued multifunction with respect to an interval-valued set multifunction.

All over this section, we suppose that $\mu : \mathrm{A} \to \mathrm{P}_{kc}(\mathrm{R}_+)$ is an interval-valued set multifunction, defined by $\mu(A) = [m_1(A), m_2(A)]$, where $m_1, m_2 : \mathrm{A} \to \mathrm{R}_+$, with $m_1(\varnothing) = m_2(\varnothing) = 0$, $m_1(A) \le m_2(A)$, for every $A \in \mathrm{A}$.

Also, let $F : T \to \mathrm{P}_{kc}(\mathrm{R}_+)$ be an interval-valued multifunction, defined by $F(t) = [f_1(t), f_2(t)]$, for every $t \in T$, with $f_1, f_2 : T \to \mathrm{R}_+$, $f_1(t) \le f_2(t)$, for every $t \in T$.

Definition 14. *F is said to be:*

I. *$\overline{\mu}$-totally measurable (on (T, A, μ))* if for every $\varepsilon > 0$, there exists $P_\varepsilon = \{A_i\}_{i=\overline{0,n}} \subset \mathrm{A}, P_\varepsilon \in \mathrm{P}(T)$ such that:

(i) $\overline{\mu}(A_0) < \varepsilon$ and

(ii) $osc(F, A_i) = \sup_{t,s \in A_i} h(F(t), F(s)) < \varepsilon$, for every $i = \overline{1,n}$.

II. *$\overline{\mu}$-totally measurable on $B \in \mathrm{A}$* if $F|_B$ is $\overline{\mu}$-totally measurable on $(B, \mathrm{A}_\mathrm{B}, \mu_B)$, where $\mu_B = \mu|_{\mathrm{A}_B}$.

Remark 15. I. If F is $\overline{\mu}$-totally measurable on T , then it is $\overline{\mu}$-totally measurable on every $A \in \mathrm{A}$.

II. F is $\overline{\mu}$-totally measurable on T if and only if the functions f_1, f_2 are $\overline{m_2}$ -totally measurable in the sense of (Gould, 1965).

Definition 16. *We denote $\sigma_{F,\mu}(P)$ (or, for short, $\sigma(P)) = \sum_{i=1}^{n} F(t_i)\mu(A_i)$, for every $P = \{A_i\}_{i=\overline{1,n}} \in \mathrm{P}(T)$ and every $t_i \in A_i$, $i = \overline{1,n}$.*

I. *F is said to be Gould μ-integrable on T if the net $(\sigma(P))_{P \in (\mathrm{P}, \le)}$ is convergent in $(\mathrm{P}_{kc}(\mathrm{R}), h)$. In this case, its limit is called the Gould integral of F on T with respect to μ, denoted by $\int_T F d\mu$.*

II. *The Gould integral on a subset E of T is defined in classical manner.*

Remark 17. I. If it exists, the integral is unique.

II. If F is μ -integrable on T , then $\int_T F d\mu \in \mathrm{P}_{kc}(\mathrm{R})$, so $\int_T F d\mu = [a,b]$, where $0 \le a \le b$. In consequence, F is μ -integrable on T if and only if there exists $A = [a,b] \in \mathrm{P}_{kc}(\mathrm{R}_+)$ such that for every $\varepsilon > 0$, there exists $P_\varepsilon \in \mathrm{P}$ (T), so that for every $P = \{A_i\}_{i \in \overline{1,n}} \in \mathrm{P}(T)$ with $P \ge P_\varepsilon$ and for every $t_i \in A_i$, $i = \overline{1,n}$, we have $h(\sum_{i=1}^{n} F(t_i)\mu(A_i), A) < \varepsilon$.

III. If $\mu = \{0\}$, then F is μ -integrable on T and $\int_T F d\mu = \{0\}$.

In what follows in this paper, suppose moreover, that $F : T \to \mathrm{P}_{kc}(\mathrm{R}_+)$ is bounded (*i.e.*, there exists $M > 0$ so that $|F(t)|\,(= f_2(t)) \le M$, for every $t \in T$) and $\mu : \mathrm{A} \to \mathrm{P}_{kc}(\mathrm{R}_+)$ is of finite variation(so $\overline{\mu}(T)(= \overline{m_2}(T)) < \infty$). We now recall from (Pap *et al*.), some results that will be useful further.

Proposition 18. *F is μ -integrable on T if and only if f_1 is m_1 -integrable and f_2 is m_2 -integrable on T in the sense of (Gavriluț and Petcu, 2007),in this case,*

$$\int_T F d\mu = [\int_T f_1 dm_1, \int_T f_2 dm_2].$$

Theorem 19. *Let $\mu : \mathrm{A} \to \mathrm{P}_{kc}(\mathrm{R}_+)$ be a q-multisubmeasure. The following statements are equivalent:*

I. *F is μ -integrable on T ;*

II. *F is $\overline{\mu}$ -integrable on T ;*

III. *F is $\overline{\mu}$ -totally measurable on T .*

If $F : \mathrm{A} \to \mathrm{P}_{kc}(\mathrm{R}_+)$ is μ -integrable we consider the set multifunction $\varphi : \mathrm{A} \to \mathrm{P}_{kc}(\mathrm{R}_+)$, defined by

$$\varphi(A) = \int_A F d\mu, \forall A \in \mathrm{A}.$$

In (Pap *et al*., submitted for publication) we established some properties of the integral φ. Our aim is to continue this study.

In what follows, we shall understand that *a property holds almost everywhere* (*μ -ae*, for short) if the property holds everywhere excepting a set of null "measure".

Theorem 20. *Suppose* $\mu: \mathrm{A} \to \mathrm{P}_{kc}(\mathrm{R}_+)$ *is q-monotone. Let* $F,G: T \to \mathrm{P}_{kc}(\mathrm{R}_+)$ *be two interval-valued multifunctions such that* F *is* μ*-integrable (on* T*) and* $F = G$ μ*-ae. Then* G *is* μ*-integrable (on* T*) and* $\int_T F d\mu = \int_T G d\mu.$

Proof. Since μ is q-monotone, then by Remark 8, m_1, m_2 are monotone functions. We observe that $F = G$ μ-ae if and only if $f_1 = g_1$ and $f_2 = g_2$ m_2-ae. In this case, $f_1 = g_1$ and $f_2 = g_2$ m_1-ae. Since F is μ-integrable, then by Proposition 18, f_1 is m_1- integrable and f_2 is m_2-integrable.

Then g_1 is m_1- integrable, g_2 is m_2- integrable and $\int_T f_1 dm_1 = \int_T g_1 dm_1$, $\int_T f_2 dm_2 = \int_T g_2 dm_2$ (these statements easily follows by means of the induced set multifunction $\mu: \mathrm{A} \to \mathrm{P}_{kc}(\mathrm{R}_+)$, $\mu(A) = [0, m(A)]$, for every $A \in \mathrm{A}$, where $m: \mathrm{A} \to \mathrm{R}_+$ is a monotone set function in Theorem 5.3 (Precupanu *et al*., 2010). In consequence, by Proposition 18, G is μ-integrable. Moreover, $\int_T F d\mu = \int_T G d\mu.$

Theorem 21. *Let* μ *be a q-multisubmeasure and* $F, G: T \to \mathrm{P}_{kc}(\mathrm{R}_+)$ *be* μ*-integrable on* T*. Then:*

I. G is φ*-integrable on* T (*where* $\varphi(A) = \int_A F d\mu, \forall A \in \mathrm{A}$);

II. $\int_T G d\varphi = \int_T FG d\mu.$

Proof. Since μ is a q-multisubmeasure, then m_1 and m_2 are submeasures. Let be $\varphi_1 = \int_T f_1 dm_1$ and $\varphi_2 = \int_T f_2 dm_2$. Since by Theorem 19, F is μ-integrable if and only if it is $\overline{\mu}$-totally measurable, by the definitions and Remark 10-III, it follows that f_1 is $\overline{m_1}$-totally measurable and f_2 is $\overline{m_2}$-totally measurable. According to Theorem 2.16 (Gavriluț and Petcu, 2007), for a real function, Gould integrability with respect to a submeasure is equivalent to its total-measurability, so f_1 is m_1- integrable and f_2 is m_2- integrable. Then by (Gavriluț and Petcu, 2007), g_1 is φ_1- integrable, g_2 is φ_2- integrable and $\int_T g_k d\varphi_k = \int_T f_k g_k dm_k$, for $k = \overline{1,2}$. Therefore,

$$\int_T Gd\varphi = [\int_T g_1 d\varphi_1, \int_T g_2 d\varphi_2] = [\int_T f_1 g_1 dm_1, \int_T f_2 g_2 dm_2] = \int_T FGd\mu.$$

We now provide a theorem of measure change type. With this end in mind, suppose T, T' are two non-empty sets, $G: T \to T'$ is a bijective function, A is an algebra of subsets of T and $\mu: \mathrm{A} \to \mathrm{R}_+$ is a set function with $\mu(A) = 0$.

Then $\mathrm{A}' = \{A' \subseteq T'; G^{-1}(A') \in \mathrm{A}\}$ is an algebra of subsets of T' and we can define $\mu^G: \mathrm{A}' \to \mathrm{R}_+$ by $\mu^G(A') = [m_1^G(A'), m_2^G(A')]$, for every $A' \in \mathrm{A}'$, where $m_i^G: \mathrm{A}' \to \mathrm{R}_+$, $m_i^G = m_i(G^{-1}(A')), \forall A' \in \mathrm{A}'$.

Theorem 22. *Let $\mu: \mathrm{A} \to \mathrm{P}_{kc}(\mathrm{R}_+)$ be a q-multisubmeasure of finite variation. If $F: T' \to \mathrm{P}_{kc}(\mathrm{R}_+)$ is μ^G -integrable on T', then $FoG: T \to \mathrm{P}_{kc}(\mathrm{R}_+)$, defined by*

$$(FoG)(t) = [(f_1 oG)(t), (f_2 oG)(t)], \forall t \in T,$$

is μ-integrable on T and, moreover,

$$\int_{T'} Fd\mu^G = \int_T FoGd\mu.$$

Proof. One can easily check that if μ is a q-multisubmeasure of finite variation, then μ^G is a q-multisubmeasure of finite variation too. Now the conclusion follows by Proposition 18 and Theorem 2.13 (Gavriluţ and Petcu, 2007).

In the following we shall obtain some results concerning integrability on atoms.

We recall that Theorem 2.16 (Gavriluţ and Petcu, 2007) shows that totally-measurability in variation and Gould integrability are equivalent on any subset of $A \in \mathrm{A}$, when dealing with submeasures $m: \mathrm{A} \to \mathrm{R}_+$. Theorem 19 proves that a similar result holds when dealing with q-multisubmeasures. In the next result we prove that this equivalence remains valid on atoms in weaker hypothesis, *i.e.*, when μ is only null-additive and q-monotone.

Theorem 23. *Suppose $\mu: \mathrm{A} \to \mathrm{P}_{kc}(\mathrm{R}_+)$ is null-additive, q-monotone, of finite variation and $A \in \mathrm{A}$ is a q-atom of μ. Then F is μ-integrable on A if and only if F is $\overline{\mu}$ - totally measurable on A.*

Proof. According to Remark 15-II, F is $\overline{\mu}$-totally measurable if and only if f_1, f_2 are $\overline{m_2}$ -totally measurable. Since $m_1 \le m_2$ it results that f_1 is

also $\overline{m_1}$ -totally measurable. Now the statement follows by Corollary 3.7 (Gavriluț, 2011) and Proposition 18.

In what follows let T be a locally compact Hausdorff topological space, K the lattice of all compact subsets of T, B the Borel σ-algebra (*i.e.*, the smallest σ-algebra containing K) and τ the class of all open sets.

Definition 24. *$\mu : \mathrm{B} \to \mathrm{P}_{kc}(\mathrm{R}_+)$ is said to be regular if for each set $A \in \mathrm{B}$ and each $\varepsilon > 0$, there exist $K \in \mathrm{K}$ and $D \in \tau$ such that $K \subseteq A \subseteq D$ and $|\mu(D \setminus K)| < \varepsilon$.*

Remark 25. We see that μ is regular if and only if the same is m_2 in the sense of Pap (1995).

Theorem 26. *Let $\mu : \mathrm{B} \to \mathrm{P}_{kc}(\mathrm{R}_+)$ be a regular q-multisubmeasure. If $A \in \mathrm{B}$ is a q-atom of μ, there exists a unique point $a \in A$ such that $\mu(A) = \mu(\{a\})$ and $\mu(A \setminus \{a\}) = \{0\}$.*

Proof. Since μ is q-multisubmeasure, then μ is null-additive, so m_1 and m_2 are null-additive. One can easily check that m_1 and m_2 are also monotone and regular (in the sense of (Pap, 1995)). Let $A \in \mathrm{B}$ be a q-atom of μ. Then A is an atom of both m_1 and m_2. Applying Theorem 9.6 (Pap, 1995) for m_1 and m_2, respectively there exist unique points $a_1 \in A$ for m_1 and $a_2 \in A$ for m_2, respectively such that $m_1(A) = m_1(\{a_1\})$, $m_1(A \setminus \{a_1\}) = 0$ and $m_2(A) = m_2(\{a_2\})$, $m_2(A \setminus \{a_2\}) = 0$, respectively.

We shall prove that $a_1 = a_2$. Suppose this is not true, *i.e.*, $a_1 \neq a_2$. Since $a_1, a_2 \in A$, then $\{a_1\} \subseteq A \setminus \{a_2\}$. By the monotonicity of m_2 we have $m_2(\{a_1\}) \leq m_2(A \setminus \{a_2\}) = 0$. Hence, $m_2(\{a_1\}) = 0$. Since $m_1 \leq m_2$ it follows that $m_1(\{a_1\}) = 0$, which contradicts the fact that $m_1(\{a_1\}) = m_1(A) > 0$. Therefore, there is only one point $a \in A$ such that $m_i(A) = m_i(\{a\})$, $m_i(A \setminus \{a\}) = 0$, for $i = \overline{1,2}$.

Theorem 27. *Suppose $\mu : \mathrm{B} \to \mathrm{P}_{kc}(\mathrm{R}_+)$ is a regular q-multisubmeasure and $F : T \to \mathrm{P}_{kc}(\mathrm{R}_+)$. If $A \in \mathrm{B}$ is a q-atom, then F is μ-integrable on A and*

$$\int_A F d\mu = F(a)\mu(\{a\}),$$

where $a \in A$ is the single point resulting by the previous theorem.

Proof. According to Theorem 19, we prove that F is $\overline{\mu}$ -totally measurable. Indeed, by Theorem 26 there exists a unique point $a \in A$ so that $\mu(A \setminus \{a\}) = \{0\}$. Then the partition $P = \{A \setminus \{a\}, \{a\}\}$ assures the $\overline{\mu}$ -totally measurability of F on A. Applying now Proposition 18 and Theorem 4.4 (Candeloro *et al*., submitted for publication) we obtain the equality.

Corollary 28. *If T is a compact Hausdorff space, $\mu : \mathrm{B} \to \mathrm{P}_{kc}(\mathrm{R}_+)$ is a regular finitely purely atomic, q-multisubmeasure (where $T = \bigcup_{i=1}^{p} A_i$ and $A_i \in \mathrm{B}, i = \overline{1, p}$ are pairwise disjoint q-atoms of μ) and if $F : T \to \mathrm{P}_{kc}(\mathrm{R}_+)$ is μ -integrable on T, then for every $i = \overline{1, p}$, there exist unique points $a_i \in A_i$ so that $\mu(A_i \setminus \{a_i\}) = \{0\}$ and, in this case,*

$$\int_T F d\mu = F(a_1)\mu(\{a_1\}) + \cdots + F(a_p)\mu(\{a_p\}).$$

Corollary 29. (*Lebesgue Type Theorem*) *Suppose $\mu : \mathrm{B} \to \mathrm{P}_{kc}(\mathrm{R}_+)$ is a regular q-multisubmeasure. If for every $n \in \mathrm{N}$, $F_n, F : T \to \mathrm{P}_{kc}(\mathrm{R}_+)$, where $F_n = [f_n^1, f_n^2]$ are μ -integrable on an atom $A \in \mathrm{B}$ of μ and if with respect to h, $(F_n)_n$ pointwise converges to F, then*

$$\lim_{n \to \infty} \int_A F_n d\mu = \int_A F d\mu.$$

Proof. By virtue of Theorems 26 and 27, there exists a unique point $a \in A$ such that $\mu(A \setminus \{a\}) = \{0\}$ and for every $n \in \mathrm{N}$, $\int_A F_n d\mu = F_n(a)\mu(A)$ and $\int_A F d\mu = F(a)\mu(A)$. Since $(F_n)_n$ pointwise converges to F with respect to h,

$$h\left(\int_A F_n d\mu, \int_A F d\mu\right) = h(F_n(a)\mu(A), F(a)\mu(A)) \le h(F_n(a), F(a))\overline{\mu}(A) \to 0.$$

REFERENCES

Aumann R.J., *Integrals of Set-Valued Functions*, J. Math. Anal. Appl., **12**, 1-12 (1965).

Aviles A., Plebanek G., Rodriguez J., *The McShane Integral in Weakly Compactly Generated Spaces*, J. Funct. Anal., **259**, *11*, 2776-2792 (2010).

Birkhoff G., *Integration of Functions with Values in a Banach Space*, Trans. Amer. Math. Soc., **38**, *2*, 357-378 (1935).

Boccuto A., Sambucini A.R., *A Note on Comparison Between Birkhoff and Mc Shane Integrals for Multifunctions*, Real Analysis Exchange, **37**, *2*, 3-15 (2012).

Boccuto A., Sambucini A.R., *A McShane Integral for Multifunctions*, J. Concr. Appl. Math., **2**, *4*, 307-325 (2004).

Boccuto A., Candeloro D., Sambucini A.R., *A Note on Set Valued Henstock-McShane Integral in Banach (Lattice) Space Setting*, arXiv:1405.6530v1 [math. FA] 26 May 2014.

Bykzkan G., Duan D., *Choquet Integral Based Aggregation Approach to Software Development Risk Assessment*, Inform. Sci., **180**, *3*, 441-451 (2010).

Bustince H., Galar M., Bedregal B., Kolesarova A., Mesiar R., *A New Approach to Interval-Valued Choquet Integrals and the Problem of Ordering in Interval-Valued Fuzzy Set Applications*, IEEE Transaction on Fuzzy Systems, **21**, *6*, 1150-1162 (2013).

Candeloro D., Croitoru A., Gavriluț A., Sambucini A.R., *Atomicity Related to Non-Additive Integrability* (submitted for publication).

Cascales B., Rodriguez J., *Birkhoff Integral for Multi-Valued Functions*, J. Math. Anal. Appl., **297**, 540-560 (2004).

Dinghas A., *Zum Minkowskischen Integralbegriff abgeschlossener Mengen*, Math. Zeit., **66**, 173-188 (1956).

Drewnowski L., *Topological Rings of Sets, Continuous Set Functions, Integration*, I, II, III, Bull. Acad. Polon. Sci. Ser. Math. Astron. Phys., **20**, 277-286 (1972).

Fremlin D.H., *The Generalized McShane Integral*, Illinois J. Math., **39**, 39-67 (1995).

Gavriluț A., Petcu A., *A Gould Type Integral with Respect to a Submeasure*, An. Ştiint. Univ. Al. I. Cuza Iaşi, **53**, *2*, 351-368 (2007a).

Gavriluț A., Petcu A., *Some Properties of the Gould Type Integral with Respect to a Submeasure*, Bul. Inst. Polit. Iaşi, s. Mat. Mec. Teor. Fiz., **53(57)**, *5*, 121-130 (2007b).

Gavriluț A., *A Gould Type Integral with Respect to a Multisubmeasure*, Math. Slovaca, **58**, 43-62 (2008).

Gavriluț A., *A Generalized Gould Type Integral with Respect to a Multisubmeasure*, Math. Slovaca, **60**, 289-318 (2010).

Gavriluț A., *Fuzzy Gould Integrability on Atoms*, Iranian Journal of Fuzzy Systems, **8**, *3*, 113-124 (2011).

Gavriluț A., *Remarks of Monotone Set-Valued Multifunctions*, Inform. Sci., **259**, 225-230 (2014).

Gavriluț A., *Regular Set Multifunctions*, Pim Publishing House, Iaşi, 2012.

Gavriluț A., Iosif A., Croitoru, A., *The Gould Integral in Banach Lattices*, Positivity (2014), DOI:10.1007/s11117-014-0283-7.

Gould G.G., *On Integration of Vector-Valued Measures*, Proc. London Math. Soc., 15, 193-225 (1965).

Guo C., Zhang D., *On Set-Valued Fuzzy Measures*, Inform. Sci., **160**, 13-25 (2004).

Hu S., Papageorgiou N., *Handbook of Multivalued Analysis*, Vol. **I**, Theory. Mathematics and its Applications, 419, Kluwer Academic Publishers, Dordrecht, 1997.

Hamid M.E., Elmuiz A.H., *On Henstock-Stieltjes Integrals of Interval-Valued Functions and Fuzzy-Number-Valued Functions*, Journal of Applied Mathematics and Physics, **4**, 779-786 (2016).

Jang L.C., *A Note on the Monotone Interval-Valued Set Function Defined by the Interval-Valued Choquet Integral*, Commun. Korean Math. Soc., **22**, 227-234 (2007).

Jang L.C, *A Note on Convergence Properties of Interval-Valued Capacity Functionals and Choquet Integrals*, Inform. Sci., **183**, 151-158 (2012).

Jang L.C., *Interval-Valued Choquet Integrals and their Applications*, J. Appl. Math.Comput., **16**, 429-445 (2004).
Jang L.C., *On Properties of the Choquet Integral of Interval-Valued Functions*, J. Appl. Math. (2011), Article ID 492149, 10 pages, DOI:10.1155/2011/492149.
Jang L.C., *The Application of Interval-Valued Choquet Integrals in Multicriteria Decision aid*, J. Appl. Math. & Computing, **20**, *1-2*, 549-556 (2006).
Li L.S., Sheng Z, *The Fuzzy Set-Valued Measures Generated by Fuzzy Random Variables*, Fuzzy Sets Syst., **97**, 203-209 (1998).
Li J., Mesiar R., Pap E., *Atoms of Weakly Null-Additive Monotone Measures and Integrals*, Inform. Sci., **257**, 183-192 (2014).
Pap E., *Null-Additive Set Functions*, Kluwer Academic Publishers, Dordrecht-Boston-London, 1995.
Pap E., Iosif A., Gavriluţ A., *Integrability of an Interval-Valued Multifunction with Respect to an Interval-Valued Set Multifunction* (submitted for publication).
Precupanu A., Croitoru A., *A Gould Type Integral with Respect to a Multimeasure* I, An. Ştiinţ. Univ. "Al. I. Cuza" Iaşi, **48**, 165-200 (2002).
Precupanu A., Croitoru A., *A Gould Type Integral with Respect to a Multimeasure* II, An. Ştiinţ. Univ. "Al. I. Cuza" Iaşi, **49**, 183-207 (2003).
Precupanu A., Gavriluţ A., Croitoru A., *A Fuzzy Gould Type Integral*, Fuzzy Sets and Systems, **161**, 661-680 (2010).
Precupanu A., Satco B., *The Aumann-Gould Integral*, Mediterr. J. Math., **5**, 429-441 (2008).
Qin J., Liu X., Pedrycz W., *Multi-Attribute Group Decision Making Based on Choquet Integral Under Interval-Valued Intuitionistic Fuzzy Environment*, International Journal of Computational Intelligence Systems, **9**, *1*, 133-152 (2016).
Sipos J., *Integral with Respect to a Pre-Measure*, Math. Slovaca, **29**, 141-155 (1979).
Sofian-Boca F.N., *Another Gould Type Integral with Respect to a Multisubmeasure*, An. Ştiinţ. Univ. "Al.I. Cuza" Iaşi, **57**, 13-30 (2011).
Spaltenstein N., *A Definition of Integrals*, J. Math. Anal. Appl., **195**, 835-871 (1995).
Tan C., Chen X., *Interval-Valued Intuitionistic Fuzzy Multicriteria Group Decision Making Based on VIKOR and Choquet Integral*, Journal of Applied Mathematics (2013), Article ID 656879, 16 pages, http://dx.doi.org/10.1155/2013/656879.
Weichselberger K., *The Theory of Interval-Probability as a Unifying Concept for Uncertainty*, Int. J. Approx. Reason., **24**, 149 -170 (2000).
Zadeh L.A., *Probability Measures of Fuzzy Events*, J. Math. Anal. Appl., **23**, 421-427 (1968).

INTEGRABILITATE ÎN CAZUL MULTIFUNCŢIILOR (DE MULŢIME) CU VALORI INTERVAL

(Rezumat)

Recent, am propus un nou tip de integrală a unei multifuncţii cu valori interval în raport cu o multifuncţie de mulţime cu valori interval. În această lucrare, continuăm studiul acestui tip de integrală, stabilind diferite proprietăţi specifice ale acesteia. De asemenea, discutăm unele proprietăţi referitoare la integrabilitatea de tip Gould pe atomi.